SERBIAN ACADEMY OF SCIENCES AND ARTS
СРПСКА АКАДЕМИЈА НАУКА И УМЕТНОСТИ

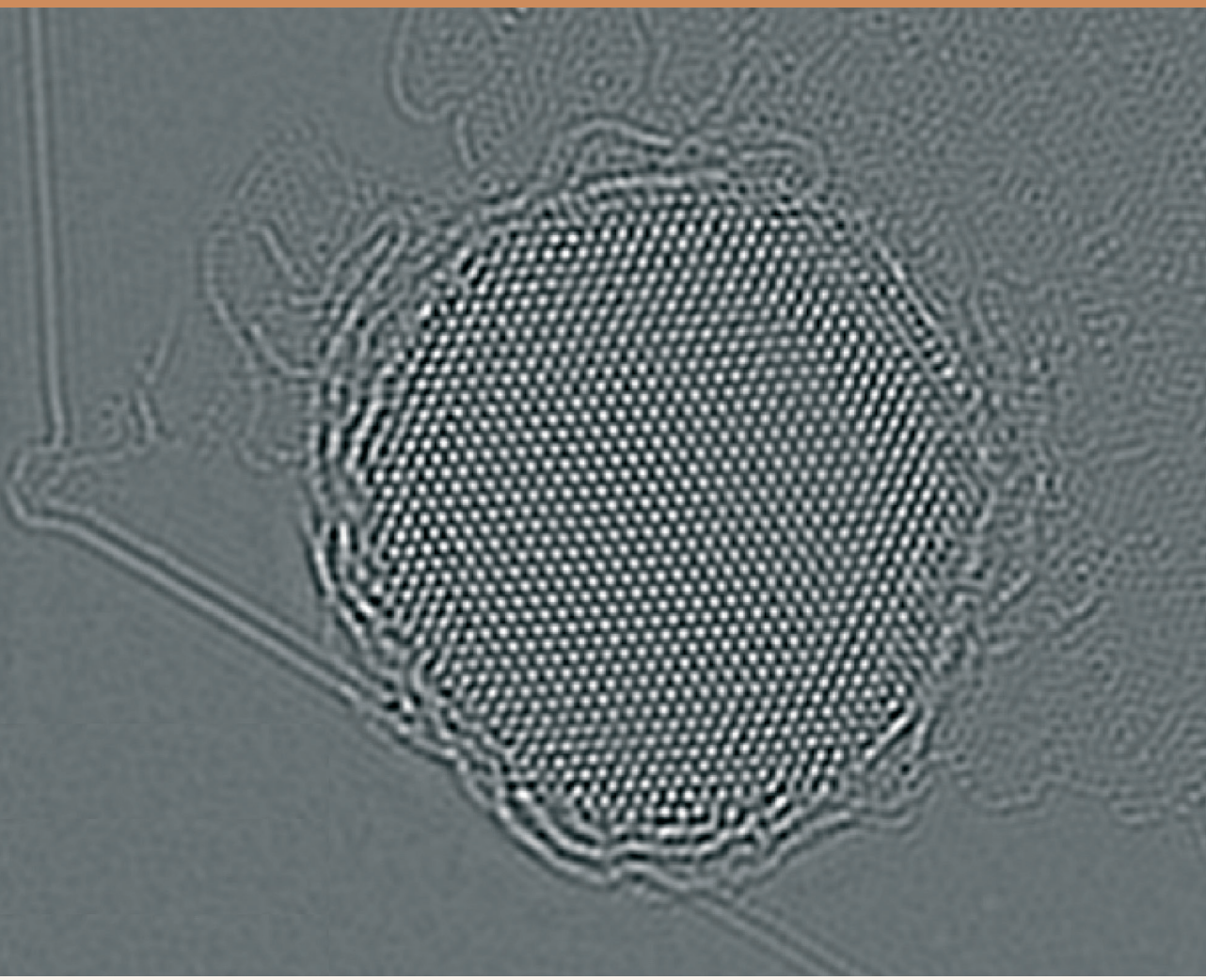

FASCINATING WORLD OF NANOSCIENCES AND NANOTECHNOLOGIES
ФАСЦИНАНТНИ СВЕТ НАНОНАУКА И НАНОТЕХНОЛОГИЈА

FASCINATING WORLD OF NANOSCIENCES AND NANOTECHNOLOGIES

ФАСЦИНАНТНИ СВЕТ НАНОНАУКА И НАНОТЕХНОЛОГИЈА

СРПСКА АКАДЕМИЈА НАУКА И УМЕТНОСТИ

ЦИКЛУС ПРЕДАВАЊА

Књига 6

ФАСЦИНАНТНИ СВЕТ НАНОНАУКА И НАНОТЕХНОЛОГИЈА

Примљено на I скупу Одељења техничких наука,
одржаном 22. јануара 2020. године

Уредници
ВЕЛИМИР Р. РАДМИЛОВИЋ
Српска академија наука и уметности
и
ЏЕФ Т. М. ДЕХОСОН
Холандска краљевска академија наука и уметности

БЕОГРАД 2020

SERBIAN ACADEMY OF SCIENCES AND ARTS

LECTURE SERIES

Book 6

FASCINATING WORLD OF NANOSCIENCE AND NANOTECHNOLOGY

Accepted at the 1st meeting of the Department of Technical Sciences
held on January 22, 2020

Editors
VELIMIR R. RADMILOVIĆ
Serbian Academy of Sciences and Arts
and
JEFF TH. M. DEHOSSON
Royal Netherlands Academy of Arts and Sciences

BELGRADE 2020

Published by
Serbian Academy of Sciences and Arts
Belgrade, 35 Kneza Mihaila St.

Reviewers
Prof. Dr. Dragan Uskoković
Prof. Dr. Djordje Janaćković

Copy editing for English
Jelena Mitrić and Vuk V. Radmilović

Proofreader
Nevena Đurđević

Translation of Summaries
Vuk V. Radmilović

Technical editor
Nikola Stevanović

Print run
400 copies

Printed by
Planeta print

ISBN 978-86-7025-859-4

Издаје
Српска академија наука и уметности
Београд, Кнеза Михаила 35

Рецензенти
Проф. др Драган Ускоковић
Проф. др Ђорђе Јанаћковић

Лектура
Јелена Митрић и Вук В. Радмиловић

Коректура
Невена Ђурђевић

Превод резимеа
Вук В. Радмиловић

Технички уредник
Никола Стевановић

Тираж
400 примерака

Штампа
Планета принт

ISBN 978-86-7025-859-4

CONTENTS

FASCINATING WORLD OF NANOSCIENCE AND NANOTECHNOLOGY

Researchers whose work has led to significant discoveries, looking much further, beyond the immediate resolution of technical problems, are asking themselves important questions such as: why individual phenomena occur, how they develop, and why they work. In order to enhance our knowledge about the world around us, and to see pictures of worlds that elude the human eye, through history many experimental and theoretical methods have been developed and are still being improved, including the development of telescopes and microscopes, which enable us to see "very large" and "very small" things.

Researchers involved in the "big things" (the universe, galaxies, stars and planets) have found that a galaxy of an average size of about 100.000 light-years has, on average, around one quadrillion (10^{15}) stars. Researchers involved in the "little things" (nanostructures, molecules, clusters of atoms, individual atoms, atomic defects, etc.) have discovered that 1 cm3 of aluminum alloys also contains approximately one quadrillion (10^{15}) nanoparticles that strengthen these alloys in order to be utilized as a structural material for aircrafts, without which modern transport is unimaginable. How do we count the number of stars in a galaxy or the number of nanoparticles in an aluminum alloy? Relatively easy, because we can see the nanoparticles in aluminum alloys using electron microscopes, and stars in a galaxy using telescopes. Scientific discoveries form the basis for scientific and technological progress, and one such example are the discoveries in the fields of nanosciences and nanotechnologies.

Why is this monograph dedicated to nanosciences and nanotechnologies?

To answer this question, we must first answer the question: what are nanoscience and nanotechnology? In the inevitable *Wikipedia*, *Encyclopedia Britannica* (and any other encyclopedia), dictionaries as well as internet sources, the terms "nanoscience" and "nanotechnology" are related to the study, understanding, controlled manipulation of structures and phenomena, and the application of extremely small things, which have at least one dimension less than 100 nm. Modern aspects of nanosciences and nanotechnologies are quite new and have been developing intensively in the last twenty to thirty years, but the nanoscale substances have been used for centuries, if not millennia. Particulate pigments, for example, have been used in ancient China, Egypt, etc., several thousands of years ago. Artists have decorated windows in medieval churches using silver and gold nanoparticles of various sizes and composition, without understanding the origin of the various colors. Nanoparticles that strengthen alloys of iron, aluminum and other metals, have been used for over a hundred years, although they have not been branded with a prefix "nano", but rather called "precipitates". Scientific disci-

plines, involved in significant research activities related to nanoscience and nanotechnology, are: physical metallurgy, materials science and materials engineering, chemistry, physics, biology, electrical engineering, and so on.

Where does the prefix "nano" come from? "Nano" comes from the Greek words *νᾶνος*, which means a dwarf, indicating a dimension of one nanometer (1 nm), which represents one-billionth (10^{-9}) of a meter; Similarly, "nanosecond" (ns) denotes a billionth of a second, and so on. This sounds a bit abstract to many, but to put things into context with which we are familiar, we can mention that the diameter of a human hair, for example, is on average about 100.000 nm (10^5 nm = 100 microns = 0.1 mm), which is roughly the bottom threshold of human eye detection; Thickness of newsprint on average is also about 100.000 nm = 100 μm = 0.1 mm; Person of 2 m height is 2.000.000.000 (2×10^9) nm high. For comparison, if we assume that the diameter of a children's glass marble was 1 nm, then the diameter of the Earth would be 1 m.

When we talk about the structures of inorganic, organic and bio-nanosystems, their dimensions are as follows: Diameter of carbon atom is in the order of 0.1 nm, or one-tenth of a billionth of a meter; Single-wall carbon nanotubes have a diameter of around 2 nm, or 2 billionth of a meter; The width of the deoxyribonucleic acid (DNA) chain is also about 2 nm, or 2 billionths of a meter; Proteins, which can vary in size, depending on how many amino acids they are composed of, are in the range mainly between 2 and 10 nm, or between 2 and 10 billionths of a meter (assuming their spherical shape); Diameter of individual molecules of hemoglobin is about 5 nm, or 5 billionths of a meter.

Indeed, these are small sizes, but why should they be important, or why does size matter? When analyzing physical systems on the nanoscale, their fundamental properties change drastically. Consider the example, melting point of gold: transition temperature of solid to liquid for gold nanoparticles ~4 nm in size, is about 400°C, while the melting temperature of bulk (macroscopic) gold is 1063°C. The same can be said for other properties: mechanical properties, electric conductivity, magnetism, chemical reactivity, etc., also may be drastically changed, which means that nanosystems deviate from the laws of classical physics that describe the motion of the planets, the direction of movement of a rockets which carry satellites to explore space, etc. The base of this fascinating behavior of nanostructures are bonds between the atoms. As structures become smaller, more atoms are present on the surface, hence the ratio of the surface area to volume for these structures increases dramatically. It results in a dramatic change of physicochemical properties of nanostructures from the bulk, as well as possible appearance of quantum effects: nanoscale structures become stronger, less brittle, demonstrate enhanced optical and catalytic properties, and generally, are very different compared to the usual, macroscopic system dimensions to which we are accustomed to in everyday practice.

This monograph comprises a number of contributions which illustrate the sparkling and fascinating world of nanoscience and nanotechnology.

Nanoporous organometallic materials, that can mimic the properties of muscles upon outside stimuli, are ideal actuators, thereby offering a unique combination of low operating voltages, relatively large strain amplitudes, high stiffness and strength. These phenomena are discussed in the manuscript of J. Th. M. DeHosson and E. Detsi.

Drugs in nanodimension range will become much more efficient with reduced adverse effects. A typical example are drugs, carried by various types of nanoparticles which have been previously functionalized, so as to only recognize diseased cells which is a highly selective medical procedure on a molecular level. Besides drugs, functionalized nanoparticles can carry radioactive material or a magnetic structure, which in a strong magnetic field develop high temperatures, and destroy cancer cells. Some aspects of electron microscopy utilized in the study of biological nanostructures are discussed in the paper of A. E. Porter and I. G. Theodorou.

Increased production of nanomaterials raises concern about their safety, not only for humans but also for animals and the environment as well. Their toxicity depends on nanoparticle size, shape, surface area, surface chemistry, concentration, dispersion, aggregation, route of administration and many other factors. The review by M. Čolić and S. Tomić summarizes the main aspects of nano-toxicity in vitro and in vivo, points out relevant tests of demonstrating toxicity and explains the significance of reactive oxygen species, as the main mechanism of nanoparticle cytotoxicity and genotoxicity through the complex interplay between nanoparticles and cellular or genomic components.

Carbon nanomaterials are a large group of advanced materials that are in focus of extensive research, due to their interesting properties and versatile applicability, especially carbon nanostructures doped by covalently bonded heteroatoms (N, B, P, etc.) which leads to improved properties. This topic is discussed in the manuscript by G. Ćirić-Marjanović.

Combinations of optical, magnetic and photocatalytic properties of nanomaterials, especially those with large energy gaps, are of great interest for nanoscience and nanotechnology. One of such systems are TiO2 nanostructures with different crystal lattices and shapes (spheres, nanotubes, nanorods), either pure or hybrid, in the form of nanocomposites with matrices based on conducting polymers, which is presented in the work of Z. Šaponjić and coauthors.

Design and manufacturing of multifunctional nanomaterials is one of the most important trends in materials nanoscience, where combining nanomaterials of various characteristics, such as ferroelectrics, ferromagnetics and ferroelastics can lead to achieving adequate multifunctionality, a good example of which are multiferroic nanomaterials, presented in the work of V. Srdić and coauthors.

Materials containing crystal grains of nanodimensions can demonstrate dramatically improved properties. Theoretically as well as experimentally, it has been shown that metallic nanostructures can attain a high percentage of theoretical strength, which questions the classical definition of material strength, stated

until recently by textbooks that does not depend on size of a tested sample. Some aspects of mechanisms of formation, growth and shrinking of crystal grains are discussed in the paper of T. Radetić.

Computational methods, including first principal calculations, have been proven to be a powerful tool in allowing investigations of systems of various complexities, spatial and temporal scales. This allows for screening of a large number of systems, which is not experimentally feasible, and also the understanding of general trends which is of great importance for both theoreticians and experimentalists. The use of this concept in applications of metallic and oxide nanoparticles is described in manuscript of I. A. Pašti and coauthors.

Being aware of the importance of nanosciences and nanotechnologies and their global impact on humanity, in the autumn of 2017, Serbian Academy of Sciences and Arts launched a series of lectures dedicated to these topics from which this monograph arose. We hope that this monograph will be of interest to the reader and can serve as a motivation for creating opportunity for research to those who want to find out more about these fascinating fields of sciences and technologies.

Velimir R. Radmilović
Serbian Academy of Sciences and Arts

Jeff Th. M. DeHosson
Royal Netherlands Academy of Arts and Sciences

ФАСЦИНАНТНИ СВЕТ НАНОНАУКА И НАНОТЕХНОЛОГИЈА

Истраживачи чији је рад довео до значајних открића гледају много даље, изван непосредног решавања техничких проблема, постављају себи важна питања, као што су: зашто се дешавају одређене појаве, како се оне развијају и на који начин функционишу? Кроз историју је развијен велики број експерименталних и теоријских метода, које се и дан-данас унапређују, како бисмо обогатили знање о свету који нас окружује и могли да видимо слике светова који измичу људском оку, укључујући ту и проналазак телескопа и микроскопа, који нам омогућавају да видимо „веома велике" и „веома мале" ствари.

Истраживачи који се баве „великим стварима" (универзумом, галаксијама, звездама и планетама) установили су да једна галаксија, око 100.000 светлосних година, у просеку садржи око једну билијарду (10^{15}) звезда. Истраживачи који се баве „малим стварима" (наноструктурама, молекулима, кластерима атома, појединачним атомима, атомским дефектима итд.) установили су да 1 cm^3 легуре алуминијума садржи око једну билијарду (10^{15}) наночестица које ојачавају ту легуру, како би могла да се користи као материјал за израду ваздухоплова, без којих је савремени транспорт незамислив. Како можемо пребројати звезде у једној галаксији или наночестице у једној легури алуминијума? Релативно лако, зато што уз помоћ електронских микроскопа можемо видети наночестице у легурама алуминијума, а звезде у галаксијама уз помоћ телескопа. Научна открића представљају основу научног и технолошког напретка, а један такав пример су открића у области нанонаука и нанотехнологија.

Зашто је ова монографија посвећена нанонаукама и нанотехнологијама?

Да бисмо одговорили на ово питање најпре морамо да установимо шта су то нанонауке и нанотехнологије? Према неизбежној Википедији, Енциклопедији Британици (или било којој другој енциклопедији), речницима, као и изворима са интернета, појмови „нанонаука" и „нанотехнологија" се односе на проучавање, разумевање, контролисано манипулисање структурама и појавама, као и на примену изузетно малих честица, чија је најмање једна димензија у опсегу до 100 nm. Иако су савремени аспекти нанонаука и нанотехнологија сасвим нови и интензивно се развијају у последњих двадесет до тридесет година, облици материје на нано скали користе се већ вековима, ако не и миленијумима. На пример, одређени пигменти коришћени су још у древној Кини и Египту, пре неколико хиљада година. Уметници су украшавали прозоре на средњовековним црквама користећи сребрне и златне наночестице различите величине и састава, при чему нису знали одакле потичу разне боје. Наночестице којима се ојачавају легуре гвожђа, алуминијума и других метала, користе се већ више од сто година,

иако у њиховом називу није садржан префикс „нано", већ се обично називају „талози". Научне дисциплине које су укључене у значајне истраживачке активности у области нанонауке и нанотехнологије су: физичка металургија, наука о материјалима и инжењерство материјала, хемија, физика, биологија, електротехника, и тако даље.

Одакле потиче префикс „нано"? Префикс „нано" потиче од грчке речи *νᾶνος*, што значи патуљак, указујући тако на димензију од једног нанометра (1 nm) која представља милијардити део метра (10^{-9} m). Слично томе, „наносекунда" (ns) означава милијардити део секунде. Ово многима може звучати помало апстрактно, међутим, ствари можемо да поставимо у контекст који је нама познат, и да поменемо, на пример, да пречник власи људске косе у просеку износи 100.000 nm (10^5 nm = 100 микрона = 0.1 mm), што отприлике представља праг онога што може да се опази голим оком. Дебљина новинског папира у просеку такође износи око 100.000 nm = 100 μm = 0.1 mm. Особа висине 2 m висока је 2.000.000.000 (2×10^9) nm. Поређења ради, ако претпоставимо да је пречник дечијег кликера 1 nm, онда би пречник планете Земље износио 1 m.

Када говоримо о структурама неорганских, органских и природних наносистема, њихове димензије су следеће: пречник атома угљеника је реда величине 0.1 nm, а то је једна десетина милијардитог дела метра; једнозидне угљеничне наноцеви имају пречник од око 2 nm, а то су два милијардита дела метра; ширина ланца дезоксирибонуклеинске киселине (ДНК) такође износи око 2 nm, а то су два милијардита дела метра; пречник протеина, чија величина често варира у зависности од тога од колико се амино киселина састоје, реда је величине 2–10 nm, или између два и десет милијардитих делова метра (под претпоставком да су сферног облика); пречник појединачних молекула хемоглобина износи око 5 nm, или 5 милијардитих делова метра.

Уистину, ово су све мале димензије, али зашто би оне уопште требало да буду важне, или зашто је величина битна? Када се анализирају физички системи на нано скали, њихова основна својства се драстично мењају. Размотримо, на пример, тачку топљења злата: температура на којој наночестице злата реда величине ~4 nm прелазе из чврстог у течно стање износи око 400°C, док је температура топљења макроскопских узорака злата 1063°C. На исти начин мењају се и неке друге особине: механичке особине, електрична проводљивост, магнетизам, хемијска реактивност итд. могу драстично да се промене, што значи да наносистеми одступају од закона класичне физике који описују кретање планета, правац кретања ракета које носе сателите за истраживање свемира итд. Ово фасцинантно понашање наноструктура потиче од веза између атома. Што су структуре мање, то је више атома присутно на површини, услед чега се однос површине и запремине ових структура драстично повећава. Као последица јавља се драматична промена физичко-хемијских својстава наноструктура у односу на структуре макроскопских димензија, као и могућа појава квантних ефеката: структуре на нано скали

постају чврше, мање крте, показују боља оптичка и каталитичка својства, и, уопштено, веома се разликују од структура уобичајених, макроскопских димензија, које сусрећемо у свакодневној пракси.

Ова монографија садржи низ радова који илуструју фасцинантан свет нанонаука и нанотехнологија.

Нанопорозни органометални материјали, који могу да опонашају особине мишића изложених спољашњим подстицајима, идеални су покретачи, који нуде јединствену комбинацију малих радних напона, релативно велике амплитуде напрезања, велику крутост и снагу. Ове појаве су описане у раду чији су аутори Ц. Т. М. ДеХосон и Е. Детси.

Лекови у области нанодимензија ће постати много ефикаснији и са смањеним штетним ефектима. Типичан пример су лекови које преносе различити типови наночестица, а које су претходно функционализоване тако да препознају само оболеле ћелије, што представља високо селективан поступак на молекуларном нивоу. Поред лекова, функционализоване наночестице могу да буду носачи радиоактивног материјала или магнетних структура, који у јаком магнетном пољу развијају високе температуре и тако уништавају ћелије рака. Одређени аспекти електронске микроскопије који се користе у проучавању биолошких наноструктура описани су у радовима чији су аутори А. Е. Портер и И. Г. Теодору.

Повећана производња наноматеријала изазива забринутост везану за њихову безбедност, не само по здравље људи, већ и за животиње и животну средину. Њихова токсичност зависи од величине наночестица, њиховог облика, величине и хемије површине, концентрације, дисперзије, склоности ка стварању агломерата, начина примене, као и многих других фактора. Рад чији су аутори М. Чолић и С. Томић даје преглед главних аспеката нанотоксичности ин витро и ин виво, указује на релевантне тестове за утврђивање токсичности, појашњава значај реактивности молекула кисеоника, као главног механизма цитотоксичности и генотоксичности наночестица кроз сложено међудејство наночестица и ћелијских или генских компоненти.

Угљенични наноматеријали представљају велику групу напредних материјала, који због својих занимљивих својстава и широке примењивости заузимају централно место у опсежним истраживањима, нарочито када су у питању угљеничне наноструктуре допиране разнородним атомима, повезаних ковалентним везама (N, B, P итд.), што доводи до побољшања њихових својстава. Ову тему обрађује рад чији је аутор Г. Ћирић-Марјановић.

Комбинације оптичких, магнетских и фотокаталитичких својстава наноматеријала, нарочито оних са великим енергијским процепом, од велике су важности за нанонауке и нанотехнологије. Један од таквих система су TiO_2 наноструктуре са различитим кристалним решеткама и облицима (наносфере, наноцеви, наноштапићи), у чистом или хибридном облику, у облику нанокомпозита са основама које су на бази проводних полимера, што је представљено у раду З. Шапоњића и сарадника.

Пројектовање и производња мултифункционалних наноматеријала представљају један од најважнијих трендова у нанонауци о материјалима, где комбиновање наноматеријала који поседују различита својства, попут фероелектричности, феромагнетизма и фероеластичности, може довести до постизања одговарајуће мултифункционалности, чији су добар пример мултифероични наноматеријали, који су представљени у раду В. Срдића и сарадника.

Материјали који садрже кристална зрна нанодимензија показују знатно побољшане особине. Теоријски и експериментално је показано да металне наноструктуре могу да достигну висок проценат теоријске чврстоће, што доводи у питање класичну дефиницију чврстоће материјала, којом се, до скоро, у уџбенцима наводило да не зависи од величине испитиваног узорка. У раду Т. Радетић разматрани су неки аспекти механизама формирања, раста и смањивања кристалних зрна.

Показало се да рачунарске методе, укључујући ту и прорачуне на бази првог принципа, представљају моћну алатку која омогућава истраживање система различитих комплексности, како на димензионој тако и на временској скали. Оне омогућавају и преглед великог броја система, што експериментално није изводљиво, као и разумевање општих трендова који су од великог значаја, како за теоретичаре тако и за експериментаторе. Коришћење овог концепта у примени металних и оксидних наночестица описане су у раду чији су аутори И. А. Пашти и сарадници.

Свесна значаја нанонаука и нанотехнологија, као и њиховог глобалног утицаја на човечанство, Српска академија наука и уметности је у јесен 2017. године покренула серију предавања посвећену овим темама, на основу којих је настала и ова монографија. Надамо се да ће ова монографија бити занимљива читаоцу и да ће моћи да послужи као мотивација за стварање прилика за истраживања онима који желе да сазнају нешто више о овим фасцинантним областима наука и технологија.

Велимир Р. Радмиловић
Српска академија наука и уметности

Џеф Т. М. ДеХосон
Краљевска холандска академија наука и уметности

PROBING THE OPTICAL, MAGNETIC AND PHOTOCATALYTIC PROPERTIES OF DOPED TIO_2 NANOCRYSTALS AND POLYMER-BASED NANOCOMPOSITES FOR VARIOUS APPLICATIONS

MARIJA RADOIČIĆ[1], MILA VRANJEŠ[1], JADRANKA KULJANIN JAKOVLJEVIĆ[1], GORDANA ĆIRIĆ MARJANOVIĆ[2], ZORAN ŠAPONJIĆ*[1]

A b s t r a c t. – This research paper focuses on doped TiO_2 nanocrystals of different shape, size and structures, in addition to nanocomposites consisting of TiO_2 nanocrystals and conductive polymers (Polyaniline (PANI)). The primary objective of this research paper is to ensure understanding of the influence of size, shape, structure and doping level on optical and magnetic properties of TiO_2 nanoparticles, as well as the interaction between nanoparticles and PANI due to the creation of desired photocatalytic properties of nanocomposites.

The doping of TiO_2 nanocrystals with rare earth ions opens up the possibility of controlling their optical properties. The Sm^{3+} doped TiO_2 faceted nanocrystals exhibited red photoluminescence, associated with $^4G_{5/2}$-^6H_J (J=5/2, 7/2 and 9/2) *f–f* transitions of Sm^{3+} in the $4f^5$ configuration, after band-to-band excitation, confirming the accomplishment of energy transfers.

The Ni^{2+} doped TiO_2 nanocrystals enabled the synthesis of optically transparent nanostructured films that showed room-temperature ferromagnetism with almost closed loop (H_C ~ 150-200 Oe) and saturation magnetization in the range of 10^{-3}-$5x10^{-2}$ μ_B/Ni depending on dopant concentration. Ni^{2+} ions that substitute core Ti atoms were found to participate in the light excitation processes, too.

The improvement of photocatalytic efficiency of TiO_2 nanocrystals by surface modification with carbonized form of PANI was tested in degradation processes of Rhodamine B and Methylene blue. The carbonized PANI/TiO_2 nanocomposites showed significantly higher photocatalytic efficacy compared to the bare TiO_2 and the non-carbonized PANI/TiO_2 nanocomposites. Their photocatalytic activity is influenced by their surface and crystalline structures, absorption coefficient in the visible part of the spectrum, high mobility of charge carriers and finally by the molecular structures of the organic dyes used.

Keywords: nanoscience, doped TiO_2, optical and magnetic properties, nanocomposites, photocatalysis, carbonized polyaniline

*Corresponding author: <saponjic@vin.bg.ac.rs >; [1]"Vinča" Institute of Nuclear Sciences, University of Belgrade, National Institute of the Republic of Serbia, P. O. Box 522, 11001 Belgrade, Serbia; [2]Faculty of Physical Chemistry, University of Belgrade, Serbia

INTRODUCTION

According to the EU adopted definition, 'nanomaterial' means a natural, incidental or manufactured material containing particles, in an unbound state or as an aggregate (collection of weakly bound particles where the resulting external surface area is similar to the sum of the surface areas of the individual components) or as an agglomerate (a particle comprising of strongly bound or fused particles) and where, for 50% or more of the particles in the number size distribution, one or more external dimensions is in the size range 1-100 nm [1]. Nanoscience, on the other hand, implies the study of nanomaterials that exhibit remarkable properties, functionality and phenomena. The fact that electronic, optical, magnetic and photocatalytic properties as well as crystalline structure of nanoparticles depends on their size, shape, surface structure and presence of dopants open up practically unlimited possibilities for innovations in terms of their various applications.

Two well-known phenomena that appear as a consequence of nanometer dimensions refer to metals and semiconductors. Namely, the changes that can be observed in metal nanoparticles refer to modification in their optical characteristics. Optical properties of metal nanoparticles are a matter of their size, shape and composition [2]. As a result of the appearance of localized surface plasmon resonance after interaction with the incident light, the absorption characteristics as well as the Rayleigh scattering of metal nanoparticles begin to depend on their shape and size. From that reason, for example, the color of spherical gold nanoparticles varies from orange, over green, and so on to pale yellow depending on the size [3], while the color of silver nanoparticles changes from red to blue, etc. if their dimension is reduced in the range below 100 nm. Such optical properties of metal nanoparticles can be exploited for imaging in biological systems and optoelectronics devices [4].

Another striking feature of nanometer-sized materials is observed in the semiconductors. In II-VI and III-V semiconductors a quantization effect that implies an increase in their band gap energy with decreasing particle size is noticed. In particular, if particle dimensions are less than the Bohr radius of exciton that range from 1 to 10 nm depending on semiconductor, an increase of their band gap energy will be observed [5]. This will result in a change in their electronic and optical properties, which will be reflected, among others, in the different position of the fluorescence maximum compared to bulk materials. In general, the maximum fluorescence is shifted to higher energies with the reduction of the nanoparticles dimensions. Semiconductor nanoparticles, the so-called quantum dots, can be of great importance as a substitute for standard histological markers in biological systems, providing greater resolution, higher intensity and emission lifetime.

Titanium (IV) oxide (TiO_2) has been one of the most studied nanomaterials, in addition to the aforementioned quantum dots and metal nanoparticles, ever since the time when Fujishima and Honda demonstrated the possibility of

photo-electrolysis of water on TiO_2 electrodes [6]. TiO_2 is a semiconductor with relatively wide band gap (3.2-3.4 eV), high transparency (λ_{abs} < 390-400 nm) and relatively high refractive index (~ 2.5). Most often occurs in three crystalline forms (anatase, rutile, brookite) and rarely in the fourth (monoclinic TiO_2 B). TiO_2 is one of the earliest studied n-type semiconductor photocatalysts that has been widely used in environmental purification, self-cleaning, H_2 production, photosynthesis, CO_2 reduction, organic synthesis, dye sensitized solar cells, etc. [7-11]. The fact that TiO_2 absorbs in the UV range, below 400 nm, significantly influences their application.

This review article focuses on wide band gap TiO_2 (non-doped/doped) nanocrystals of different shape (spherical, tubular, rod-like), size, and structures (crystalline and surface) as well as on hybrid materials-nanocomposites consisting of these nanocrystals and conductive polymer Polyaniline (PANI).

To understand size, shape, structure and doping level influence the inherent optical and magnetic properties of TiO_2 nanoparticles, as well as the interaction between nanoparticles and polymer matrix (PANI), which occurs upon the creation of the desired photocatalytic properties of nanocomposites have been the main research objectives.

TIO_2 NANOCRYSTALS DOPED WITH TRANSITION AND RARE EARTH METALS

Optical properties of Sm^{3+} doped TiO_2 nanocrystals

Doping or introducing impurities/ions into semiconductor materials is usually performed in order to control some of their properties. According to the classical model of nucleation, the main obstacles to the success of this process are: the non-competitiveness of the nucleation of doped and non-doped nanocrystals from the kinetic aspect and a more favorable reaction path leading to the formation of a critical nucleus consisting of pure material. For example: 2% of Co^{2+} ions eliminates about 35% of nucleation events during the synthesis of ZnO due to an increase in the activation energy and critical radius of nucleation [12]. On the other hand, according to Norris et al. who studied Mn doped II–VI and IV–VI nanocrystals, doping efficiency is determined by three main factors: surface morphology, nanocrystal shape, and surfactants in the growth solution [13]. Their kinetics-based model predicts that impurities will be incorporated into nanocrystals only if they can bind to their surface during growth, for a period of time comparable to reciprocal growth rate. The binding energy of dopant ions adsorbed at certain level determines the retention time and in particles that are smaller than 2 nm there is no effective doping. These authors also found that the diffusion of dopant ions within the nanocrystal had no role, and that it was possible on the surface.

Taking into account all these findings our approach for obtaining high quality TiO_2 nanocrystals of different shapes and sizes doped with rare earth (Sm^{3+}, Eu^{3+}) and transition metal ions (Mn^{2+}, Ni^{2+}, Cu^{2+}) rests on the use of titania nanotubes as precursor. The synthesis of TiO_2 doped nanoparticles by solution chemical route, hydrothermally, through shape transformation using dispersions of titania nanotubes in the presence of dopant ions as a precursor opened up the possibility for the elimination of driving force problems that arise from the increase in the activation energy for nanocrystal nucleation in the presence of the dopant ions and its consequent exclusion during nanoparticle growth [14]. Besides the shape transformation during the hydrothermal synthesis of doped TiO_2 nanoparticles, structural reorganization also occurs. We found that titania nanotubes were ideal starting materials for reshaping because of the adequate ratio of surface and bulk (interior and exterior) coordinatively unsaturated Ti sites [14]. Those coordinatively unsaturated Ti sites generally appear as an accommodation of objects in the nanoscale regime for high curvature and surface reconstruction [15]. Anatase TiO_2 nanocrystallites of various sizes and shapes could be synthesized using the hydrothermal process and nanotubes as a precursor simply by changing the concentration of nanotubes, pH of suspension, temperature and time of autoclaving [16]. Scrolled titania nanotubes are characterized by a large fraction (40%) of highly reactive undercoordinated interior and exterior Ti atoms [17]. A strong adsorption of dopant ions at undercoordinated sites that terminate layers of scrolled TiO_2 nanotubes before hydrothermal treatment results in the formation of doped TiO_2 nanoparticles.

In Fig. 1 a conventional TEM image of open-ended scrolled TiO_2 nanotubes used as a precursor for the synthesis of doped TiO_2 nanoparticles is shown. The TEM image at higher magnification, inset, revealed multiwall morphology, diameter of ~10 nm, inner diameter ~7 nm and inter-wall spacing of about 0.73 nm. The length of nanotubes varies up to several hundred nm.

Single doping of TiO_2 nanocrystals with rare earth ions opens up the possibility of controlling the optical properties by the band gap structure of the semiconductor host. In general, TiO_2 is a suitable host material for rare earth ions, the so-called phosphor materials, due to a large band gap, high refractive index and lower phonon energy (less than 700 cm^{-1}). The rare earth doped semiconductors are of interest in optical devices applications such as LEDs, displays, and optical communications [18] as well as bio labels [19].

The Sm^{3+} doped TiO_2 nanoparticles were synthesized by hydrothermal treatment of dispersion of TiO_2 nanotubes in the presence of samarium ions with the goal to sensitize Sm^{3+} ions by energy transfer from the crystal lattice of host (TiO_2) after its band-to-band excitation. Such energy transfer is achievable due to the low phonon energy of TiO_2 and the higher energies of defect states in TiO_2 than $^4G_{5/2}$ emitting level in Sm^{3+}.

TEM micrographs of polyhedral 0.4 at.% Sm^{3+} doped TiO_2 nanoparticles, Fig. 1b, clearly show a relatively uniform size distribution in the range of 12-14 nm. On a high-resolution TEM image, Fig. 1c, high crystallinity can be perceived.

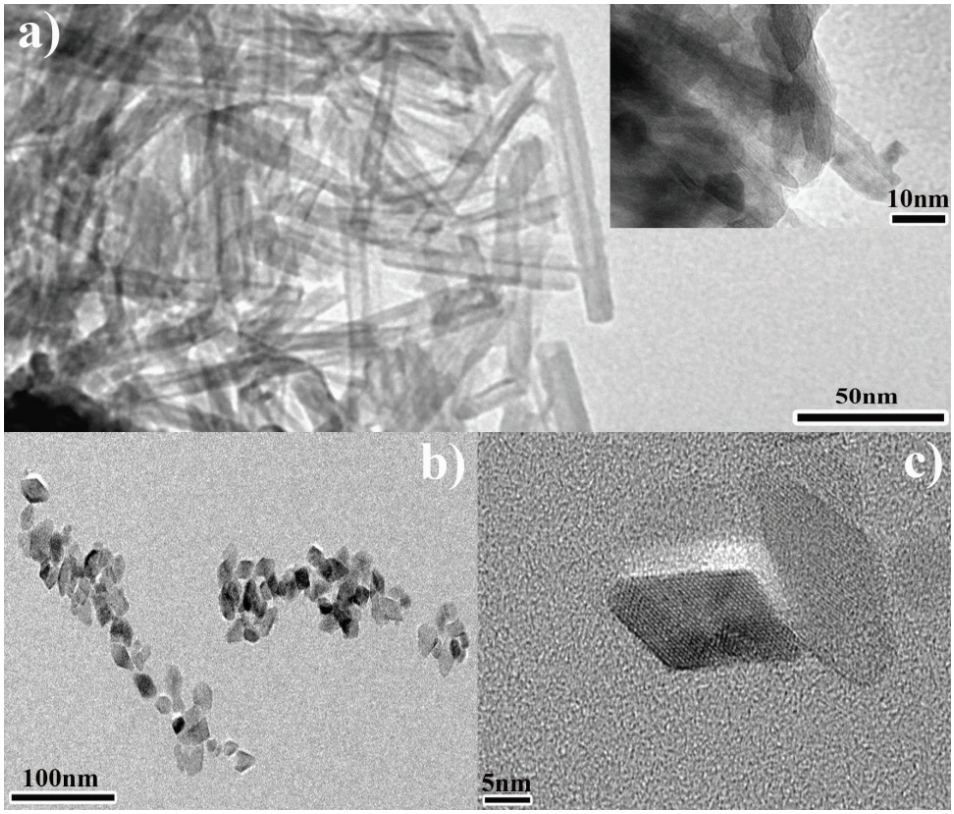

Figure 1. TEM images (a) of titania nanotubes. Inset: at higher magnification, (b) 0.4 at% Sm^{3+} doped TiO_2 nanoparticles, and (c) 0.4 at% Sm^{3+} doped TiO_2 nanoparticles at higher magnification. (Reprinted from Journal of Luminescence Vol. 143, M. Vranješ, J. Kuljanin-Jakovljević, S. P. Ahrenkiel, I. Zeković, M. Mitrić, Z. Šaponjić, J. M. Nedeljković, Sm^{3+} doped TiO_2 nanoparticles synthesized from nanotubular precursors-luminescent and structural properties, pages: 453–458, Copyright (2013), with permission from Elsevier).

X-ray diffractograms, Fig. 2, revealed the homogeneous anatase TiO_2 crystalline form of Sm^{3+} doped TiO_2 nanoparticles, with characteristic diffraction peaks that retained the corresponding intensity ratio, regardless of dopant concentration [20]. Other crystalline phases were not detected. Substitution of Ti^{4+} ion (r_{ion}= 0.964Å) in anatase crystal lattice with the Sm^{3+} ion (r_{ion}= 0.78Å) induced the increase of *a* and *c* dimensions of elemental cell as well as its volume [20].

After excitation of TiO_2 nanoparticles (E >3.2 eV), the following relaxation processes of photoinduced charge carriers occur: a) de-excitation of the electrons to the bottom of the conduction band; b) electrons detained by defects near the conduction band; c) thermal excitation from the crystal lattice defects; e) de-excitation of electrons to luminescent defects; f) non-radiative recombination process. It is

known that the radiative luminescence in TiO_2 is rather weak while the nonradiative charge-recombination path is dominant, due to the strong coupling of wave functions of the trapped electrons and trapped holes with lattice phonons [21].

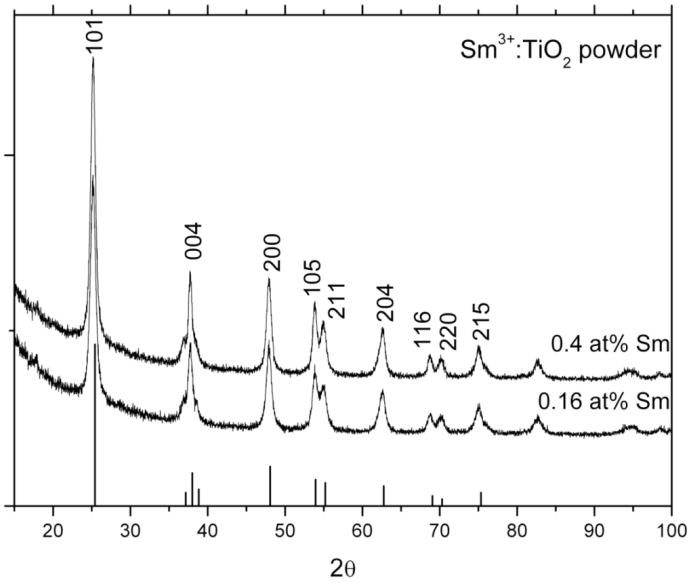

Figure 2. XRD spectra of undoped, 0.16 and 0.4 at% Sm^{3+} doped TiO_2 nanoparticles. Bragg peak positions, Miller indices, and peak intensities for anatase TiO_2 are included for reference. (Reprinted from Journal of Luminescence Vol. 143, M. Vranješ, J. Kuljanin-Jakovljević, S. P. Ahrenkiel, I. Zeković, M. Mitrić, Z. Šaponjić, J. M. Nedeljković, Sm^{3+} doped TiO_2 nanoparticles synthesized from nanotubular precursors-luminescent and structural properties, pages: 453–458, Copyright (2013), with permission from Elsevier).

In Fig. 3a, the photoluminescence spectra of undoped TiO_2 nanoparticles after excitation at λ_{exc}=365 nm is shown.

Broad and poorly structured emission spectrum with band centered at λ~450 nm is characteristic of TiO_2, an indirect semiconductor, containing various defects (lattice, surface and oxygen vacancies).

With the aim of confirming energy transfer from the TiO_2 host to Sm^{3+}, the photoluminescence spectra of 0.16 and 0.4 at% Sm^{3+} doped TiO_2 nanoparticles after band to band excitation (λ_{exc}=365 nm) were measured, Fig. 3b. For Sm^{3+} ions in the $4f^5$ configuration, orange-red emission as a consequence of $^4G_{5/2}$-^6H_J (J=5/2, 7/2 and 9/2) *f–f* transitions is distinctive [19, 22, 23, 24, 25]. In the spectra in Fig. 3b three well-resolved emission bands that appear at 582, 612 and 662 nm due to $^4G_{5/2}\rightarrow{}^6H_{5/2}$, $^4G_{5/2}\rightarrow{}^6H_{7/2}$, and $^4G_{5/2}\rightarrow{}^6H_{9/2}$ crystal-field transitions, respectively, implied the insertion of Sm^{3+} ions into quite regular environment [22]. The most pronounced transitions, as expected according to the selection rule ΔJ=±1,

is $^4G_{5/2} \rightarrow {}^6H_{7/2.}$ The luminescence lifetime of $^4G_{5/2}$ of Sm^{3+} determined by monitoring emission decay of the $^4G_{5/2} \rightarrow {}^6H_{7/2}$ transition at 612 nm, is 970 μs. The use of titania nanotubes as a precursor in hydrothermal process for the synthesis of Sm^{3+} doped TiO_2 nanoparticles have opened up the possibility for host-sensitized photoluminescence upon band gap excitation to be observed.

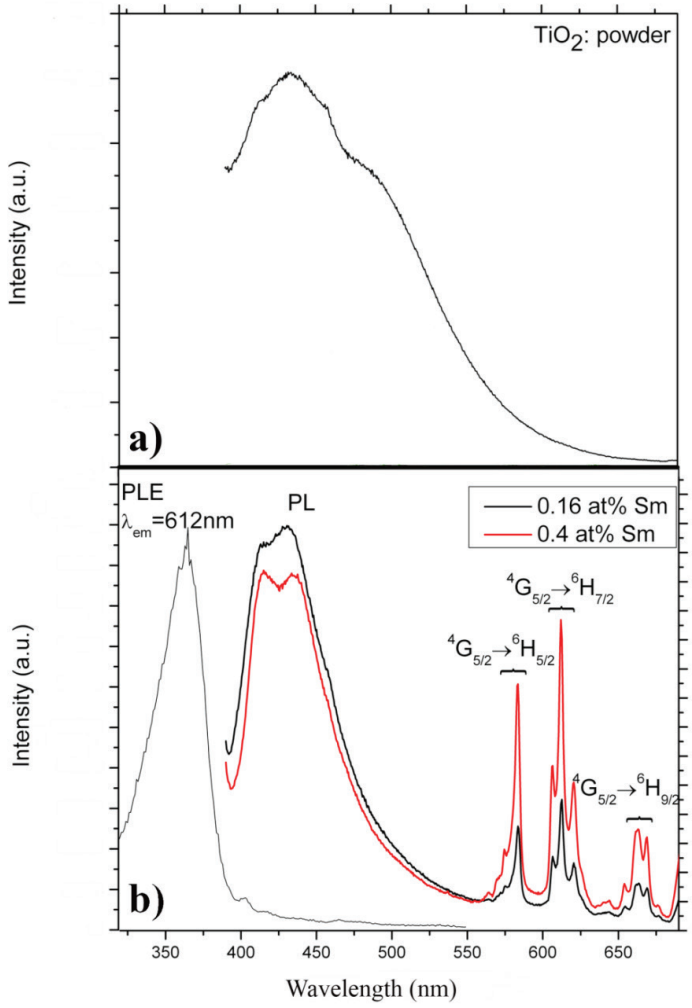

Figure 3. (a) PL spectrum of bare TiO_2 nanoparticles, (b) PL spectra of 0.16 and 0.4 at% Sm^{3+} doped TiO_2 nanoparticles (λ_{exc}=365 nm) and PLE spectrum of 0.4 at% Sm^{3+} doped TiO_2 nanoparticles (λ_{em}=612 nm). (Reprinted from Journal of Luminescence Vol. 143, M. Vranješ, J. Kuljanin-Jakovljević, S. P. Ahrenkiel, I. Zeković, M. Mitrić, Z. Šaponjić, J. M. Nedeljković, Sm^{3+} doped TiO_2 nanoparticles synthesized from nanotubular precursors-luminescent and structural properties, pages: 453–458, Copyright (2013), with permission from Elsevier).

Magnetic properties of Ni^{2+} doped TiO_2 nanocrystals

Theoretical considerations have proved that doped metal oxides can be considered as another viable candidate for diluted magnetic semiconductors (DMS), besides the well-known III-V and II-VI semiconductors. Room-temperature ferromagnetism (Curie temperatures higher than room temperature) has been detected in wide band metal oxides (TiO_2, ZnO) doped with transition metal ions (Co, Cu, Mn) [26–32]. The advantage of using single-crystalline DMS nanoparticles in comparison to polycrystalline or bulk DMS is in lower probability of defect formation and the agglomeration of dopants within DMS [33, 34]. This class of nanoscale materials can be used as a component of spintronic devices enabling simultaneous control of charge and spin.

In this study the hydrothermal synthesis of Ni^{2+} doped TiO_2 nanocrystals that exhibit room-temperature ferromagnetism, using the dispersions of titania nanotubes at different pHs as precursors, was reported. The conventional TEM images of titania nanotube precursors and the Ni^{2+} doped TiO_2 nanoparticles synthesized at pH=3 and p=H 5 are shown in Fig. 4. The diameter of nanotubes is about 10 nm, Fig. 4a, while the Ni^{2+} doped TiO_2 nanoparticles synthesized at pH=3 are characterized by uniform size (d~20 nm) and shape, Fig. 4b. On the other hand, the TEM image of Ni^{2+} doped TiO_2 nanocrystals synthesized at pH=5 reveals their different dimensions and various shapes (polygonal and rod-like), Fig. 4c [34]. The SAED patterns shown in Figs. 4b and c, have confirmed the anatase crystalline structure of Ni^{2+} doped TiO_2 nanocrystals independently of applied synthesis conditions.

It is known that doping of TiO_2 nanocrystals with transition metal ions causes the red shift of absorption as a consequence of possible charge transfer [35, 36]. In addition, the substitution of Ti ions with dopant of different valence induces the formation of oxygen vacancies within TiO_2 crystalline structure [34], then structure relaxation in DMSs and consequently enhanced magnetic properties. More precisely, enhanced magnetic properties come from the role of oxygen vacancies as a mediator of exchange interaction between magnetic dopant atoms. Namely, the electrons associated with defects in oxides occupy large Bohr orbital and tend to form an impurity band mixing with the 3d states of dopant ions, allowing ferromagnetic coupling [37].

In order to confirm the integration of Ni^{2+} within TiO_2 nanocrystals the optical properties of powdered samples of the 0.25 at% and 1.48 at% Ni^{2+} doped TiO_2 nanocrystals as well as bare TiO_2 nanocrystals were measured in a reflection mode, Fig. 5 (34). The red shift of absorbance observed for both doped TiO_2 samples confirmed that electronic states of dopant atoms were coupled to the band structure of TiO_2 nanoparticles [14].

An X-ray diffraction pattern (not shown) confirmed the anatase crystal structure of Ni^{2+} doped TiO_2 nanoparticles independently of dopant concentration that varied from 0.09 to 1.80 at% [34].

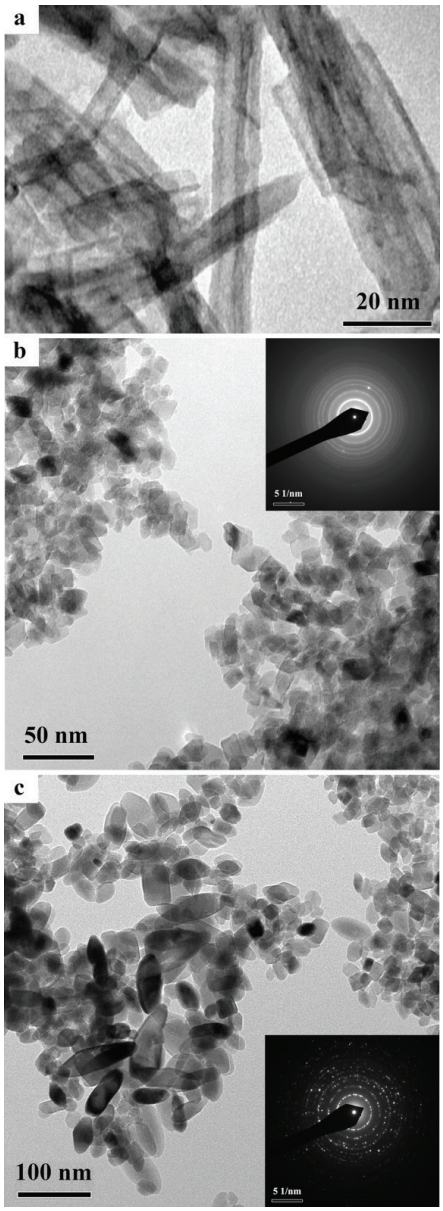

Figure 4. TEM images of titania nanotubes (a), 0.25 at% Ni^{2+} doped TiO_2 nanoparticles synthesized at pH 3; Inset: SAED pattern (b), and 1.48 at% Ni^{2+} doped TiO_2 nanoparticles synthesized at pH 5; Inset: SAED pattern (c). (Reprinted from Journal of Alloys and Compounds, Vol. 589, M. Vranješ, Z. Konstantinović, A. Pomar, J. Kuljanin Jakovljević, M. Stoiljković, J. M. Nedeljković, Z. Šaponjić, Room-temperature ferromagnetism in Ni^{2+} doped TiO_2 nanocrystals synthesized from nanotubular precursors, Pages 42–47, Copyright (2014), with permission from Elsevier).

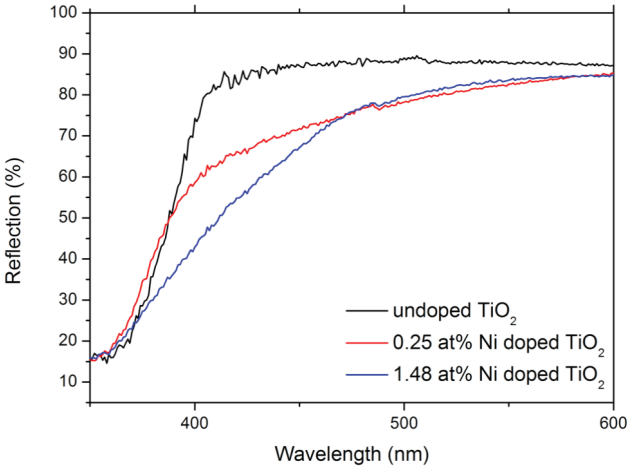

Figure 5. Reflection spectra of powders of 0.25 and 1.48 at% Ni^{2+} doped TiO_2 nanocrystals and bare TiO_2 nanoparticles. (Reprinted from Journal of Alloys and Compounds, Vol. 589, M. Vranješ, Z. Konstantinović, A. Pomar, J. Kuljanin Jakovljević, M. Stoiljković, J. M. Nedeljković, Z. Šaponjić, Room-temperature ferromagnetism in Ni^{2+} doped TiO_2 nanocrystals synthesized from nanotubular precursors, Pages 42–47, Copyright (2014), with permission from Elsevier).

The room-temperature field dependence of the magnetic moments of films made of 0.09, 0.25, 0.86, 1.48 and 1.8 at% Ni^{2+} doped TiO_2 nanoparticles, after diamagnetic corrections are shown in Fig. 6.

Weak ferromagnetic behavior was observed in all samples, with coercive field of H_c ~ 200 Oe for the samples made of 0.09 and 0.25 at% Ni^{2+} doped TiO_2 nanoparticles synthesized at pH 3, Fig. 6a. On the other hand, ferromagnetic ordering with coercive field of H_c ~ 150 Oe for the samples made of 0.86, 1.48 and 1.80 at% Ni^{2+} doped TiO_2 nanoparticles synthesized at pH 5, Fig. 6b, were also observed [34]. Room-temperature ferromagnetic ordering with saturation magnetic moment in the range of 10^{-3}-$5x10^{-2}$ μ_B per Ni atom was noticed for all measured films made of Ni^{2+} doped TiO_2 nanoparticles. The saturation magnetization observed in samples synthesized at pH=3, Fig. 6a, decreases with increasing Ni content. The observed loss of magnetization could be caused by the exchange interaction among Ni atoms incorporated in the nanoparticle or the absence of ordering of Ni atoms within anatase crystalline lattice [34]. In the samples of 1.48 and 1.80 at% Ni^{2+} doped TiO_2 nanocrystals synthesized at pH=5, the saturation magnetization values are one order of magnitude lower than that of the samples synthesized at pH=3 (0.09 and 0.025 at%). The cause of the decrease of saturation magnetization with dopant concentration increase, lies in different shapes of nanoparticles synthesized at pH=3 and pH=5. In other words, the presence of rod-like particles in the samples synthesized at pH 5 might be an additional reason for the lower values of magnetization compared to the doped nanoparticles without shape

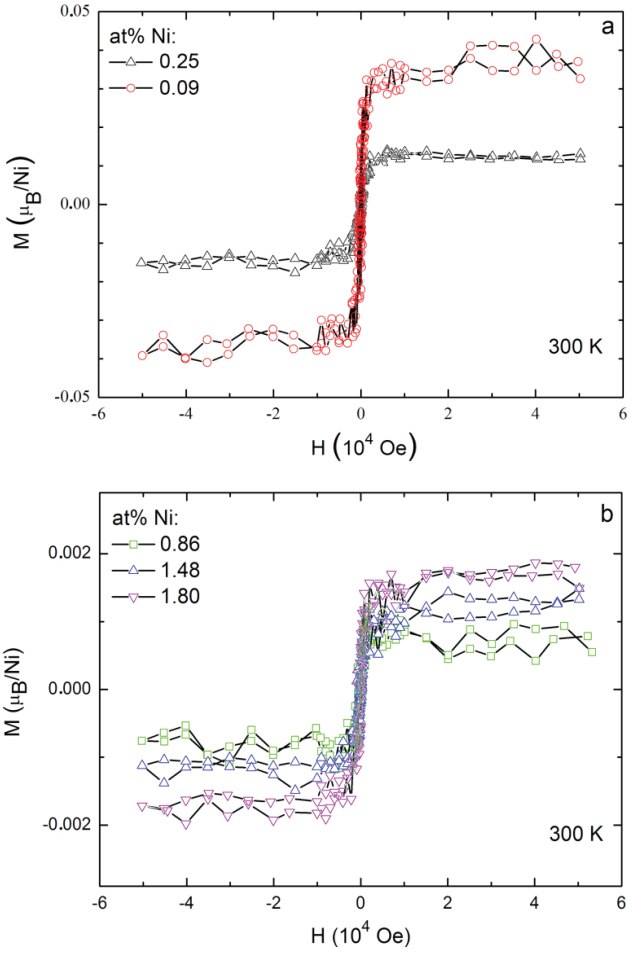

Figure 6. Isothermal magnetizations of the films made of 0.09 and 0.25 at% Ni^{2+} doped TiO_2 nanoparticles synthesized at pH 3 (a) and 0.86, 1.48 and 1.80 at% Ni^{2+} doped TiO_2 nanocrystals synthesized at pH 5 (b). (Reprinted from Journal of Alloys and Compounds, Vol. 589, M. Vranješ, Z. Konstantinović, A. Pomar, J. Kuljanin Jakovljević, M. Stoiljković, J. M. Nedeljković, Z. Šaponjić, Room-temperature ferromagnetism in Ni^{2+} doped TiO_2 nanocrystals synthesized from nanotubular precursors, Pages 42–47, Copyright (2014), with permission from Elsevier).

anisotropy, synthesized at pH 3 [34, 38, 39]. Since the oxygen vacancies within crystalline structure of doped nanoparticles are donor type defects, the observed larger saturation magnetization could be justified by their role of a mediator of the exchange interaction between magnetic dopant atoms [34]. Taking into account higher surface to volume ratio of Ni^{2+} doped TiO_2 nanocrystals synthesized at pH 3 (0.09 and 0.25 at% of dopant ions), due to their uniform morphology (size and

shape), one could expect a larger number of interfacial defects/oxygen vacancies in these samples in comparison to all samples synthesized at pH 5 (0.86, 1.48 and 1.80 at% Ni^{2+} doped TiO_2 nanocrystals) [34]. Assuming random orientation of rode-like Ni^{2+} doped TiO_2 nanocrystals within nanoparticle films, the projection of the magnetization vectors along the field direction will be probably lower [34].

This synthetic approach opened up the possibility for the synthesis of TiO_2 nanocrystals doped with various transition metal ions that shows room-temperature ferromagnetic ordering [40, 41, 42].

PHOTOCATALYTIC PROPERTIES OF CARBONIZED PANI/TIO$_2$ NANOCOMPOSITES

It is the photocatalytic activity of TiO_2, particularly in the degradation processes of organic molecules on the surface of TiO_2 nanocrystals that this material is well-known for. Photocatalytic reactions on TiO_2 are driven by photo-excited electron-hole pairs generated upon light irradiation of TiO_2 nanocrystals with energy equal to or greater than its *Eg*~3.2 eV.

These photogenerated electron–hole pairs may further migrate to the surface of semiconductor where they could be involved in photocatalytic reactions. Redox reactions ensue once photogenerated electrons reach the electron acceptors such as O_2, while the holes reach donors (e.g. H_2O and OH^-) that have been adsorbed on the surface of the semiconductor photocatalysts. Together, these highly oxidant species contribute to the heterogeneous photocatalytic decomposition of organic pollutants [43, 44].

The relatively large band-gap of TiO_2 nanoparticles (3.0–3.2 eV) limit their optical absorption to the ultraviolet (UV) part of the solar spectrum that accounts for ~ 5% of the solar irradiation received on the earth. Given the aforementioned observation, the question always arises as to how to improve the photocatalytic efficiency of nanocrystalline TiO_2. There are several pathways leading to the solution of this problem as follows: a) doping with different ions that would be positioned in a band gap, from an energy point of view, thus contributing to the excitation of electrons with energy lower than 3 eV; b) coupling of TiO_2 nanocrystals with visible light-responsive n-type semiconductor such as for example CdS forming CdS/TiO_2 heterojunction. Due to the suitable positions of the conductive and valence bands of CdS in relation to the positions of those in TiO_2, it is possible to expect an efficient charge separation and charge transfer, which leads to a reduced recombination and finally towards an increase in the overall photocatalytic efficiency of TiO_2.

Our approach to solving the problem concerning the insufficient efficiency of TiO_2 nanocrystals included the modification of TiO_2 nanoparticles with a conductive polymer, PANI, i.e. the synthesis of nanocomposites [45]. The aim was to take advantage of conductive properties of PANI that was in direct contact,

electronically coupled, with TiO_2, and would contribute to the increased separation efficiency of photogenerated charges in TiO_2 [46–48]. PANI is one of the most commonly used conductive polymers and has the following characteristics: possess own conductivity due to the extended π conjugation of the basic chain, thermal stability and reversibility between doped and neutral states. In addition, PANI is an efficient electron donor and a hole acceptor. Its structure consists of benzenoid amines and quinonoid imines. Otherwise, this polymer may have different redox or acid-base forms. Owing to the fact that PANI is N-containing polymer, it can be utilized to produce a new class of 1-D nanostructured N-containing carbon materials electronically coupled with TiO_2 that can be expected to be even more efficient in charge separation processes on the surface of photo-excited TiO_2 nanocrystals. In general, a nanocomposite comprising N-containing carbonaceous material and TiO_2 nanocrystals is very simply synthesized by carbonization process of PANI/TiO_2 nanocomposites at 650°C in an inert atmosphere [49–51].

It is well known that the significant improvement in photocatalytic activity of TiO_2 is achieved when it is in contact with graphene structures, but preparation procedure of these nanocomposites is not straightforward.

In order to avoid a more complex synthetic method for applying graphene to the surface of TiO_2 nanocrystals, in this study we explored the influence of carbonization of polyaniline in the presence of TiO_2 nanocrystals on their photocatalytic activity. The photocatalytic efficiency of these nanocomposites was compared with bare TiO_2 nanocrystals and non-carbonized PANI/TiO_2 nanocomposites following degradation process of model molecules: Methylene blue and Rhodamine B.

Carbonized PANI/TiO_2 nanocomposites were synthesized using non-carbonized PANI/TiO_2 nanocomposite powder as a precursor, in an argon atmosphere by ramping temperature up from room temperature to 650°C, holding at this temperature for 15 min, and cooling to room temperature. During the carbonization process, condensation of the rings from the PANI chains in nanocomposites results in the formation of cyclic and aromatic segments accompanied by a change in the crystal structure of the TiO_2 nanoparticles [49, 52]. Changing the crystalline structure of TiO_2 nanoparticles during carbonization at 650 °C contributes to increased photocatalytic efficiency of nanocomposites. The additional characteristic of carbonized PANI structures is the possibility for nitrogen to occupy three different positions: pyridine-like, pyrrole-like and substitutional (graphitic) like. For the conductivity of carbonized PANI forms as for charge transfer to such structures the existence of nitrogen is of great importance since it affects the electronic structure of the carbonized form [49].

Raman spectroscopy was used to confirm the carbonization efficiency and presence of TiO_2 nanocrystals as well as the possible appearance of new crystal form of TiO_2 (rutile). Raman spectra of precursor non-carbonized TP-50 nanocomposite sample (the initial [TiO2]/[ANI] mole ratio was 50) and carbonized TPC-50 nanocomposite sample, for comparison, are shown in Fig. 7.

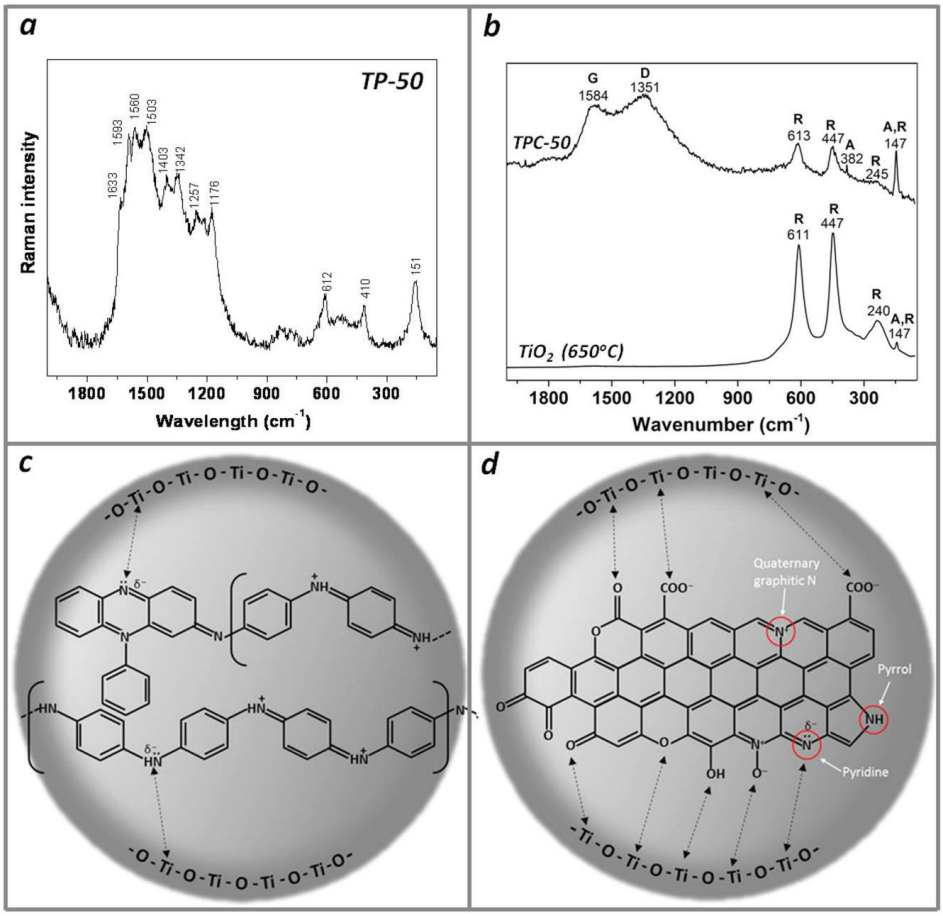

Figure 7. Raman spectra of TP-50 nanocomposite (a), TPC-50 nanocomposite (b) and bare TiO_2 NPs calcined at 650ºC (b); Schematic presentations of possible interactions between TiO_2 NPs and PANI before carbonization (c) and after carbonization (d). (Reprinted from Applied Catalysis B: Environmental, Vol. 213, M. Radoičić, G. Ćirić-Marjanović, V. Spasojević, P. Ahrenkiel, M. Mitrić, T. Novaković, Z. Šaponjić, Superior photocatalytic properties of carbonized PANI/TiO_2 nanocomposites, Pages 155–166, Copyright (2017), with permission from Elsevier).

The Raman spectrum of TP-50 nanocomposite sample, Fig. 7a, revealed emeraldine salt form of PANI whose characteristic bands were observed at: 1598, 1513, 1345 and 1172 cm^{-1} [45, 53]. The bands observed at 1569, 1410 and 617 cm^{-1}in the Raman spectrum of sample TP-50 can be associated with the presence of substituted phenazine structural units, known to be crucial for the formation of PANI nanostructures [54, 55] and as we confirmed in our previous work they were of great importance for the interaction of PANI chains and TiO_2 nanopar-

ticles utilizing free-electron coupling on nitrogen atoms [56]. The bands that appeared at 155, 421 and 617 cm^{-1}, Fig. 7b, can be assigned to the E_g phonon mode, B_{1g} and E_g modes of the anatase phase, respectively [57, 58, 59], which confirms the presence of TiO_2 nanocrystals in the nanocomposite TPC-50. In the presence of positively charged TiO_2 nanocrystals the initiation centers for polymerization process are the protonated oligoanilines. Figure 7c shows a scheme of the possible interaction between non-carbonized PANI and TiO_2 nanocrystals. On the other hand, the carbonized nanocomposite sample TPC-50 possesses completely different, i.e. more simple structure of Raman spectrum in comparison to sample TP-50. The observed spectral changes with only two bands at 1584 cm^{-1} and 1351 cm^{-1} indicated significant changes in PANI molecular structures. Taking into account that two bands at 1584 cm^{-1} and at 1351 cm^{-1} are assigned to graphitic G band and D bands, respectively, it can be concluded that carbonized PANI structure is significantly disordered [60, 61]. Disorders in molecular structure of carbonized PANI affect its electronic structure, band gap, optical properties, and conductivity, whose changes significantly influence the photoinduced charge transfer efficiency and photocatalytic activity of TPC nanocomposites [49]. Some additional changes observed in the Raman spectrum of TPC-50 refer to the appearance of new bands characteristic for the rutile TiO_2 crystalline phase. Namely, carbonization process at 650°C induced structural changes in anatase TiO_2 nanocrystals, i.e. a rutile crystalline form partial transformation. Bands at 613, 447, 245 and 147 cm^{-1} are assigned to A_{1g}, E_g, second-order (two-phonon) scattering and B_{1g} modes of rutile crystalline phase, respectively [58, 59, 62, 63]. The appearance of mixed phase (anatase/rutile) TiO_2 nanocrystals, i.e. catalytic "hot-spots" at the interface between two phases, favors photocatalytic processes [64] in the presence of TPC nanocomposites.

Figure 8 shows the TEM images of nanocomposite sample TPC-80 with the corresponding selected area diffraction pattern. An increase in TiO_2 particle size is observed. The spotty ring SAED pattern, Fig. 8b, indicates the presence of anatase and rutile crystalline structures in polynanocrystalline TPC-80 sample [64]. The TEM image at higher magnification, Fig. 8c, confirmed a uniformly deposited layer of carbonized form of PANI whose thickness is ~0.6 nm. The lattice spacing value of 0.35 nm obtained by FFT operations can be assigned to (101) direction of anatase TiO_2 [65].

The influence of carbonization process at 650°C on crystalline structure of TiO_2 nanoparticles in nanocomposites has been carefully studied on three samples with different initial [TiO_2]/[ANI] mole ratios (20, 50 and 80) using XRD measurements. Figure 9 shows the XRD patterns of bare TiO_2 nanoparticles, bare TiO_2 nanoparticles calcined at 650°C and nanocomposite samples TPC-20, TPC-50 and TPC-80.

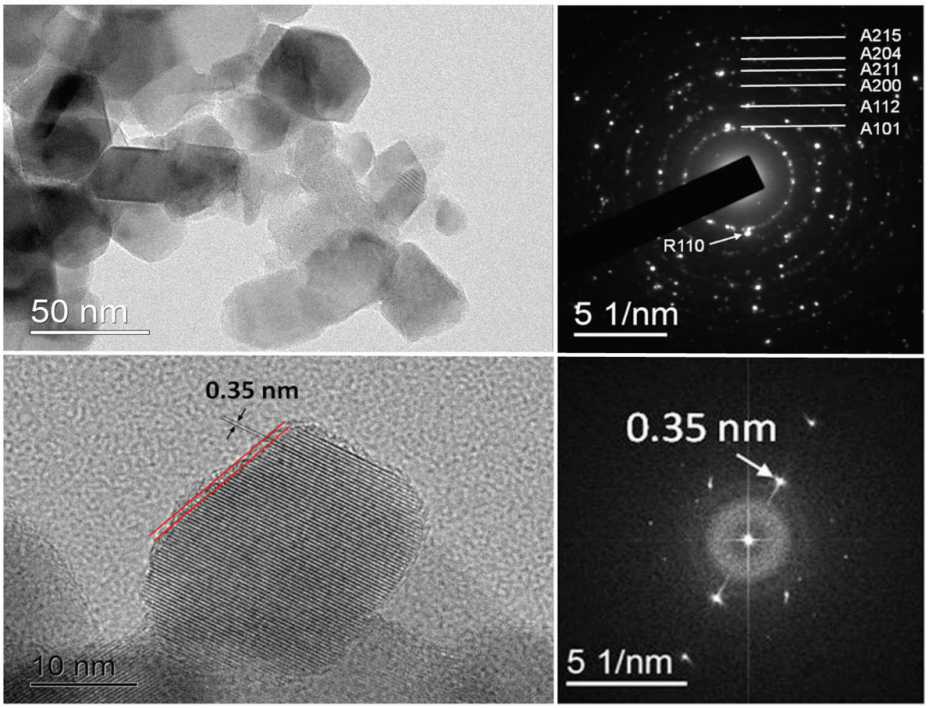

Figure 8. TEM image of TPC-80 nanocomposite sample (a), the corresponding SAED pattern (b), TEM image at higher magnification of representative anatase TiO_2 NP (c) and the corresponding FFT pattern (d). (Reprinted from Applied Catalysis B: Environmental, Vol. 213, M. Radoičić, G. Ćirić-Marjanović, V. Spasojević, P. Ahrenkiel, M. Mitrić, T. Novaković, Z. Šaponjić, Superior photocatalytic properties of carbonized PANI/TiO_2 nanocomposites, Pages 155–166, Copyright (2017), with permission from Elsevier).

It is clear from Fig. 9 that in all TPC nanocomposite samples a crystalline mixture of anatase and rutile TiO_2 nanoparticles exists independently of the amount of carbonized PANI in samples. This finding supports the changes observed in the Raman spectrum of sample TPC-50 confirming that carbonization at 650°C introduces an additional crystalline structure. All diffraction peaks characteristic of anatase phase located at: $2\theta=25.4^{o}(101)$, $37.8^{o}(004)$, $48.0^{o}(200)$, $54.5^{o}(105)$, $62.2^{o}(204)$ (JCPDS 21-1272), as well as of rutile phase located at $2\theta=27.5^{o}(110)$, $36.1^{o}(101)$, $54.4^{o}(211)$ (JCPDS 21-1276) were observed in all TPC samples. In addition, it should be pointed out that in spite of identical experimental conditions during the synthesis of TPC samples the anatase to rutile ratio was different from one sample to another. The only way this observation could be explained is by the different amount of carbonized PANI on the surface of TiO_2 nanoparticles caused by different initial aniline/TiO_2 nanoparticles mole ratio [66]. Different initial amount probably affects the different thickness of car-

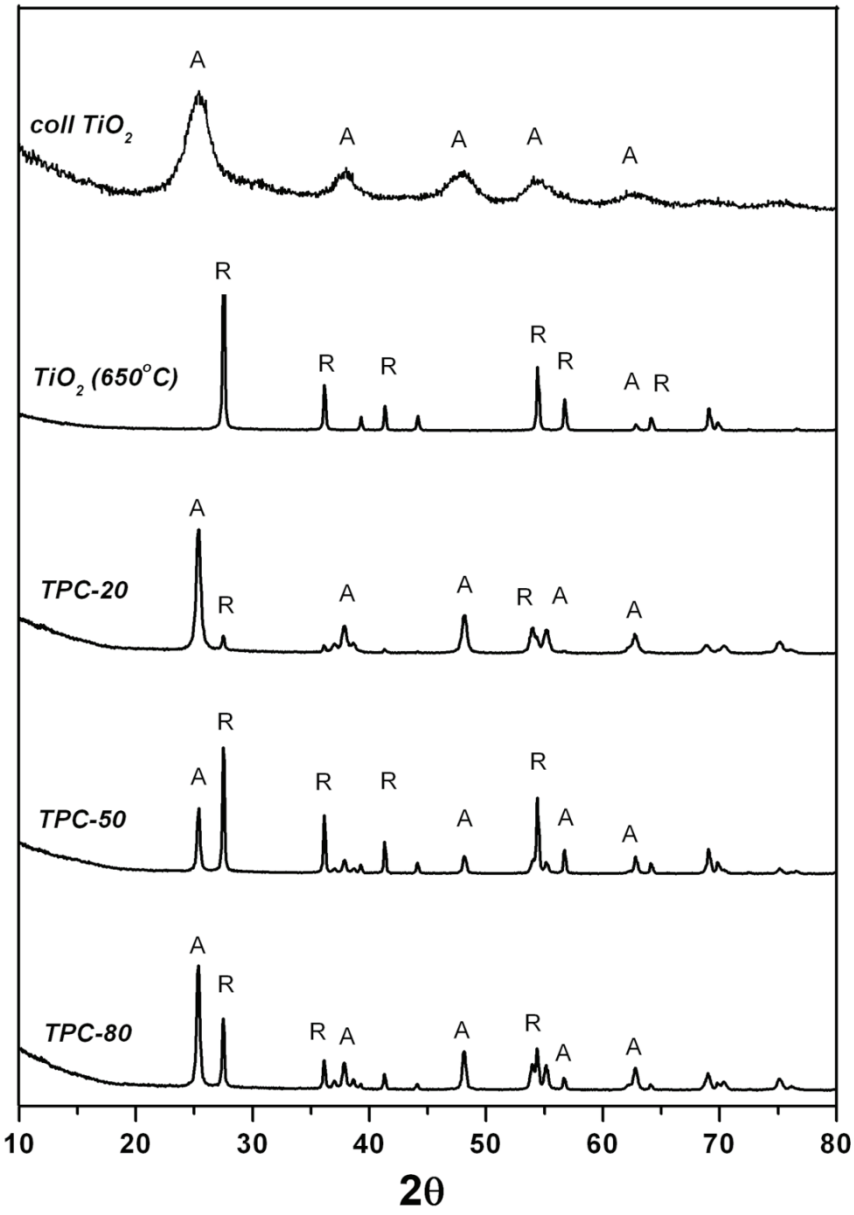

Figure 9. XRD patterns of colloidal TiO_2 NPs before and after calcination at 650°C and nanocomposite samples TPC-20, TPC-50, and TPC-80. (Reprinted from Applied Catalysis B: Environmental, Vol. 213, M. Radoičić, G. Ćirić-Marjanović, V. Spasojević, P. Ahrenkiel, M. Mitrić, T. Novaković, Z. Šaponjić, Superior photocatalytic properties of carbonized PANI/TiO_2 nanocomposites, Pages 155–166, Copyright (2017), with permission from Elsevier).

bonized PANI layer on TiO_2 nanoparticles by inducing different heat flow and consequently the changes in crystalline structure of TiO_2 during carbonization. Moreover, the thicknesses of carbonized layers in TPC samples are too tiny to be detected with XRD. On the other hand, different anatase/rutile ratio in TCP nanocomposites dovetails well with the observation that the calcination of bare TiO_2 nanoparticles at 650°C induces, almost completely, the disappearance of anatase crystalline phase (1%), Fig. 9, which confirms the role of carbonized layer on the surface of TiO_2 nanoparticles. In support of that, the largest amount of nitrogen (0.306%), among all measured samples, has been obtained for the sample TPC-20 by elemental analysis. The largest amount of nitrogen corresponds to the highest amount of carbonized PANI in that sample and consequently to the lowest percentage of rutile (<10%), as revealed [66]. In addition, there is a space for the influence of morphology and the molecular structure of PANI chains before carbonization on the anatase/rutile ratio [66].

In our previous work we successfully applied non-carbonized PANI/TiO_2 nanocomposites for the degradation of Rhodamine B and Methylene blue using white light and revealed that such nanocomposite system showed higher photocatalytic efficacy compared to bare TiO_2 NPs [45]. We concluded that photocatalytic efficacy strongly depended on the surface structure of nanocomposites, but at the same time the molecular structure of organic dyes must also be taken into account. From the photocatalytic point of view, the main objectives of the present study are the improvement of the overall photocatalytic efficiency/activity of TiO_2 nanocrystals by surface modification with carbonized PANI form and the mechanistic understanding of the photocatalytic degradation processes of model pollutant molecules. Nevertheless, the challenges that are reflected in the minimization of the electron/hole recombination in TiO_2 nanoparticles, provision of highly adsorptive active sites, achieving a uniform coating and optimum thickness of conducting polymer layers still remain.

The photocatalytic activities of TPC [20, 50, 80] nanocomposites were tested by monitoring the degradation process of dye molecules (Methylene blue and Rhodamine B) after white light illumination. As showed in Fig. 10, decreases in concentrations of dyes versus illumination time were followed spectroscopically (UV-Vis).

The sample that exhibited maximum photocatalytic efficacy in the degradation of Methylene blue is TPC-80. In the presence of this sample the degradation of Methylene blue was achieved within 60 min, Fig. 10a, while the sample TPC-50 removed 89% of MB for the same illumination period. The most inefficient system for 60 min of illumination was TPC-20. Nevertheless, it is interesting to note that sample TPC-80 is characterized by the lowest adsorption capacity (Q_{max}= 1.360 mg/g) for tested dye, while the sample TPC-20 possesses the highest specific surface area (S_{BET}= 35 m^2/g) [66]. The lowest photocatalytic activity of sample TPC-20 can be explained with the smallest pore size (4 nm) compared to other samples. For successful degradation of Methylene blue, in general, the influence of pore size was

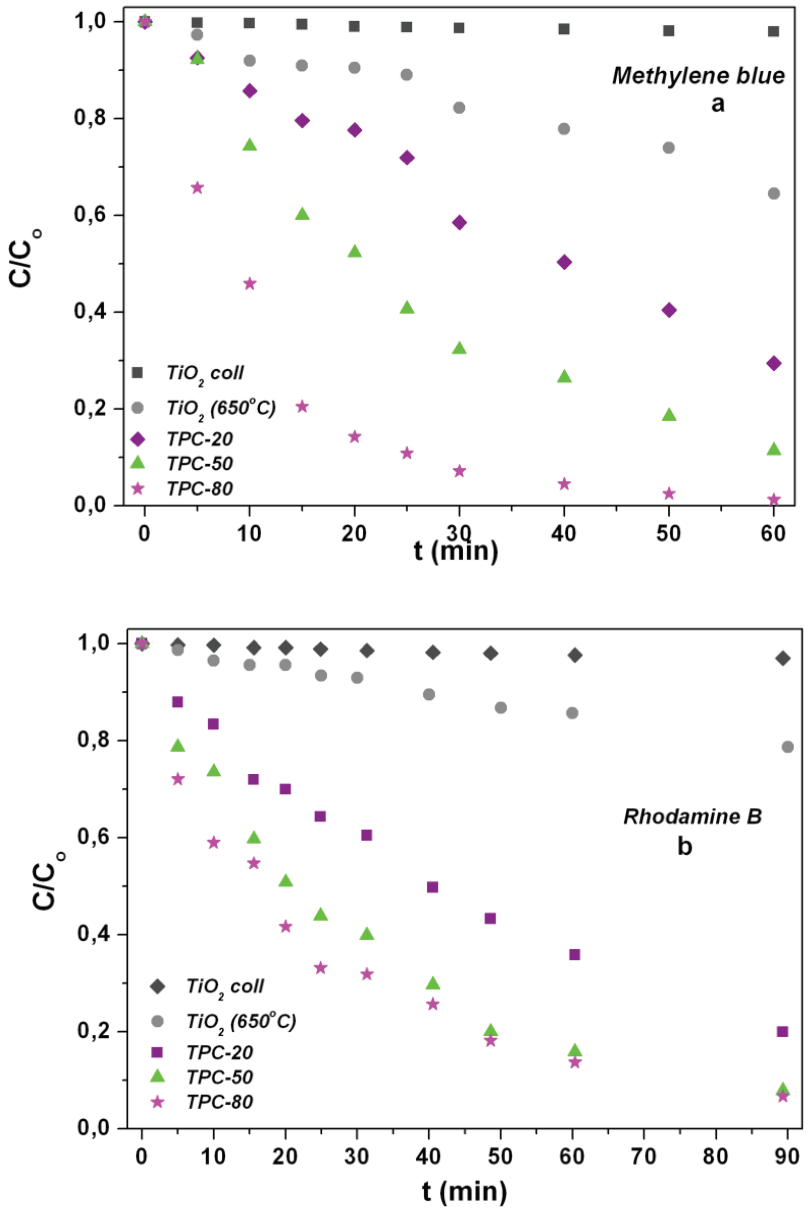

Figure 10. Changes of relative concentrations of Methylene blue (a) and Rhodamine B (b) during the photodegradation in the presence of TPC nanocomposites and bare TiO_2 NPs calcined at 650°C. (Reprinted from Applied Catalysis B: Environmental, Vol. 213, M. Radoičić, G. Ćirić-Marjanović, V. Spasojević, P. Ahrenkiel, M. Mitrić, T. Novaković, Z. Šaponjić, Superior photocatalytic properties of carbonized PANI/TiO_2 nanocomposites, Pages 155–166, Copyright (2017), with permission from Elsevier).

less important compared with the influence of interactions between dye and photocatalyst [66]. Namely, nitrogen in thiazine group of Methylene blue could ensure the efficient hydrogen-bonding interaction of N· ·H-N type with an H atom from -NH groups (e.g. from a pyrrole-type group) in TPC nanocomposites, particularly in the sample with the highest percentage of nitrogen such as TPC-80 (0.3056%), which could also lead to greater overall photocatalytic efficiency [66]. It should be mentioned here that all carbonized TPC nanocomposite samples showed significantly higher photocatalytic efficiency than non-carbonized PANI/TiO_2 nanocomposites, thereby confirming that carbonization of PANI contributes more efficiently to charge separation in photo-excited TiO_2 nanocrystals [66]. In our previous work we tested the photocatalytic degradation of Methylene blue in the presence of non-carbonized PANI/TiO_2 nanocomposites with the same initial ratio of TiO_2 nanocrystals and aniline (50:1), as in the TPC-50 sample [45]. Within 6 hours of white-light illumination, only 57% of Methylene blue degraded in the presence of non-carbonized PANI/TiO_2 nanocomposites, clearly indicating a significant increase in the degradation efficiency in the presence of a carbonized sample.

As per photocatalytic efficiencies of TPC nanocomposites in the process of degradation of Rhodamine B similar results were obtained, as shown in Fig. 10b. Namely, after 90 min of illumination, the resulting degradation efficiency varied from 80% to 96% depending on the initial ratio of TiO_2 nanocrystals and aniline in TPC nanocomposites [66]. As in the case of degradation of Methylene blue, the photocatalytic activity of non-carbonized PANI/TiO_2 samples in the degradation process of Rhodamine B was significantly lower, i.e. only 48% of Rhodamine B was degraded after 6 hours of illumination [66]. Nevertheless, carbonized PANI/TiO_2 sample, TPC-50, with the same initial ratio of TiO_2 and aniline, degraded 92% of Rhodamine B already after 90 min of illumination. A slightly greater activity during degradation process of RB demonstrated sample TPC-80 (95%, after 90 min of illumination) (66). Similar photocatalytic activities of two carbonized PANI/TiO_2 samples (TPC-50 and TPC-80) characterized with different initial TiO_2/aniline ratio could be found in their comparable pore volumes (0.095 and 0.131 cm^3/g) [66]. Larger pore volumes allow easier access of RB molecules to the surface of TPC photocatalyst, taking into account their dimension and steric hindrance, which leads to greater efficiency of photocatalytic processes [66]. The observed dominant photocatalytic activities of the sample TPC-80 in degradation processes of both dyes, MB and RB, could be also explained by the lowest level of agglomeration in this sample, as SEM characterization (not shown) revealed [66].

Significantly faster degradations of Methylene blue and Rhodamine B in the presence of various carbonized PANI/TiO_2 nanocomposites (TPC) than in the presence of bare TiO_2 nanocrystals was confirmed from the kinetic model assuming the use of low dye concentration that further allowed the application of classical first order equation. First order kinetics in the presence of TPC nanocomposites revealed a linear relationship (not shown) between the degradation rate constants (k_{app}) of Methylene blue and Rhodamine B, calculated from the

first-order kinetics, and initial TiO_2/aniline mole ratios. The reaction rate constants of Methylene blue removal via photocatalytic degradation increased from k_{app} = 0.018 min^{-1} for nanocomposite sample TPC-20, over k_{app} = 0.035 min^{-1} for sample TPC-50, to k_{app} = 0.078 min^{-1} for sample TPC-80. The reaction rate constant of Rhodamine B removal for sample TPC-20 was 0.017 min^{-1}, while for samples TPC-50 and TPC-80 reaction rate constants were 0.030 and 0.033 min^{-1}, respectively [66].

Improved photocatalytic efficiency of carbonized TPC nanocomposite samples compared to precursor non-carbonized PANI/TiO_2 nanocomposites, could be also explained by different crystalline structures of TiO_2 nanoparticles. Namely, during carbonization process of PANI the crystalline structure of TiO_2 nanoparticles is also changed resulting in the appearance of rutile crystalline form. The existence of both anatase and rutile crystalline forms of TiO_2 in the same nanocomposite sample improves the photoinduced charge separation that opens the way for more efficient photocatalytic processes. It is known that visible light induced charges in rutile TiO_2 phase are stabilized through electron transfer to lower energy anatase lattice trapping sites [64]. In this way, catalytic "hot spots" are created at the rutile-anatase interface, which lead to overall increase of titania photocatalytic activity [66]. The reason for the largest rate constants (k_{app}) observed in degradation processes of both dyes in the presence of sample TPC-80 could be find in fact that sample TPC-80 contains 38% of the rutile phase [66]. This amount of rutile is very close to reported content in mixed phase TiO_2 (Degussa commercial powder), which shows an excellent photocatalytic activity in the degradation processes of test molecules [67, 68].

In addition, to explain more efficient photoinduced charge separation in TPC nanocomposites, compared to non-carbonized PANI/TiO_2 nanocomposites, the presence of nitrogen in such carbonized nanostructures should be also taken into account, Scheme 1. In general, nitrogen doping of carbonized systems affects their electronic structures by inducing a significant increase in conductivity due to the recovery of the sp^2 graphene network disturbed by defects (disrupted conjugation sites, vacancies, etc.) [69].

The graphene-like carbonaceous materials in contact with metal-oxide semiconductors usually have a role of electron acceptors and transporters, which could improve overall photocatalytic performances of nanocomposites contributing to the decrease of charge (electron-hole pairs) recombination [66]. Wang et al. reported that the existence of nitrogen in carbonaceous structure increased the electronic density of states near the Fermi level, providing efficient electron transfer from TiO_2 nanocrystals [70]. Efficient electron transfer, on the other hand, enables the extended life time of holes, which eventually lead to higher photocatalytic efficiency of nanocomposite systems. An additional role of nitrogen in carbonized structure, such as TPC nanocomposites, is to provide anchor sites for TiO_2 nanoparticles establishing close interfacial contact between carbonized PANI and TiO_2, and further stabilizing the nanocomposite system [71, 72].

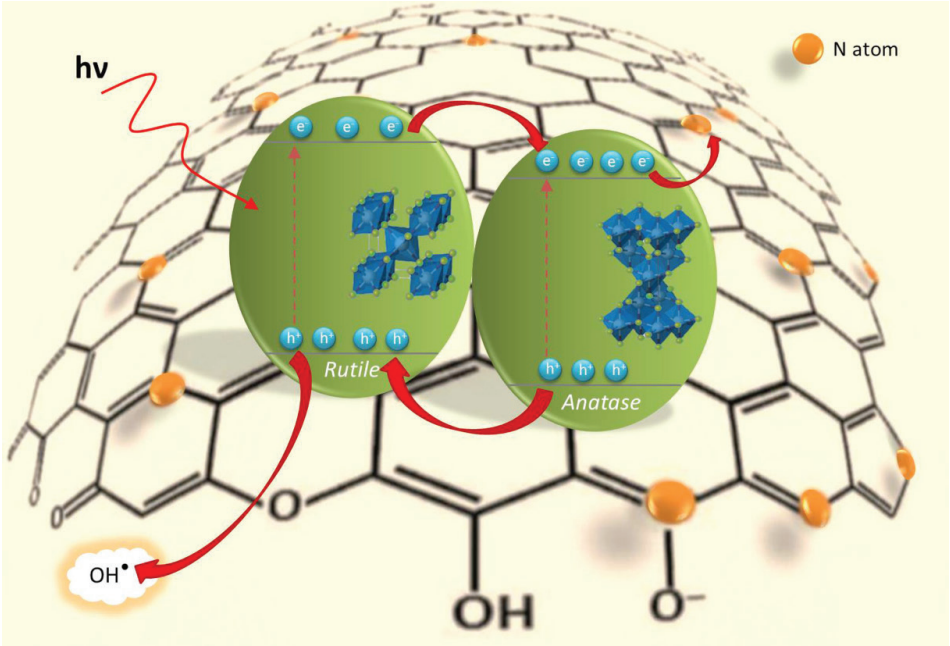

Scheme 1. Photoinduced charge separation in TPC nanocomposites. (Reprinted from Applied Catalysis B: Environmental, Vol. 213, M. Radoičić, G. Ćirić-Marjanović, V. Spasojević, P. Ahrenkiel, M. Mitrić, T. Novaković, Z. Šaponjić, Superior photocatalytic properties of carbonized PANI/TiO_2 nanocomposites, Pages 155–166, Copyright (2017), with permission from Elsevier).

SUMMARY

The obtained results revealed that the nanocomposites based on carbonized form of conductive polymer PANI and TiO_2 nanocrystals had a great potential for application in the photocatalytic degradation processes of organic pollutants. Such nanocomposite system showed significantly higher photocatalytic efficiency compared to bare TiO_2 nanocrystals and nanocomposites based on the non-carbonized form of PANI and TiO_2 nanocrystals. The optimization of carbonization process and conditions for the synthesis of non-carbonized precursors (pH, type of acid dopant, etc.) opens up the possibility to increase the photocatalytic activity of carbonized PANI/TiO_2 nanocomposites.

The hydrothermally induced shape transformation of titania nanotubes in the presence of transition metals or rear earth ions opened up numerous possibilities for the synthesis of optically or magnetically active doped TiO_2 nanocrystals of various size and shapes. This approach to the synthesis of doped samples eliminates the driving force problem that arises from the increase in the activation

energy for nanocrystal nucleation in the presence of the dopant ions and its consequent exclusion from the crystalline structure during nanoparticle growth. The shape transformation from titania nanotubes into nanoparticles in the presence of dopant ions induces structural reorganization too, while at the same time avoids the nucleation stage and problems related to it.

REFERENCES

[1] Recommendation on the definition of a nanomaterial 2011/696/EU; http://ec.europa.eu/environment/chemicals/nanotech/faq/definition_en.html.

[2] *Nanometals: formation and color*, L. M. Liz-Marzan, Elsevier, 2004.

[3] C. A. Mirkin, The Beginning of a Small Revolution, *Small* 1 (2005) 14–16. doi:10.1002/smll.200400092.

[4] *From Bioimaging to Biosensors-Noble Metal Nanoaprticles in Biodetection*, Edited by Lai-Kwan Chau and Huan-Tsung Chang, Pan Stanford Publishing, 2013.

[5] S. I. Pokutnyĭ, Excition states in semiconductor quantum dots in the modified effective mass approximation, *Semiconductors.* 41(11) (2007) 1323–1328.

[6] Fujishima, K. Honda, Electrochemical Photolysis of Water at a Semiconductor Electrode, *Nature.* 238 (1972) 37–38.

[7] Y. Ma, X. Wang, Y. Jia, X. Chen, H. Han, C. Li, Titanium Dioxide-Based Nanomaterials for Photocatalytic Fuel Generations, *Chem. Rev.* 114 (2014) 9987–10043.

[8] S. N. Frank, A. J. Bard, Heterogeneous photocatalytic oxidation of cyanide ion in aqueous solutions at titanium dioxide powder, *J. Am. Chem. Soc.* 99 (1977) 303–304.

[9] K. Koci, L. Obalova, Z. Lacny, Photocatalytic reduction of CO_2 over TiO_2 based catalysts, *Chem. Pap.* 62 (2008) 1–9.

[10] B. Kraeutler, A. Bard, Heterogeneous photocatalytic preparation of supported catalysts. Photodeposition of platinum on titanium dioxide powder and other substrates, *J. Am. Chem. Soc.* 100 (1978) 4317–43108.

[11] R. Wang, K. Hashimoto, A. Fujishima, M. Chikuni, E. Kojima, A. Kitamura, M. Shimohigoshi, T. Watanabe, Light-induced amphiphilic surfaces, *Nature.* 388 (1997) 431–432.

[12] D. A. Schwartz, N. S. Norberg, Q. P. Nguyen, J. M. Parker, D. R. Gamelin, Magnetic Quantum Dots: Synthesis, Spectroscopy, and Magnetism of Co^{2+}- and Ni^{2+}-Doped ZnO Nanocrystals, *J. Am. Chem. Soc.* 125 (2003) 13205–13218.

[13] S. C. Erwin, L. Zu, M. I. Haftel, A. L. Efros, T. A. Kennedy, D. J. Norris, Doping semiconductor nanocrystals, *Nature.* 436 (2005) 91–94.

[14] Z. V. **Š**aponjić, N. M. Dimitrijević, O. G. Poluektov, L. X. Chen, E. Wasinger, U. Welp, D. M. Tiede, X. Zuo, T. Rajh, Charge Separation and Surface Reconstruction: A Mn^{2+} Doping Study, *J. Phys. Chem. B* 110 (2006) 25441–25450.

[15] T. Rajh, L. X. Chen, K. Lukas, T. Liu, M. C. Thurnauer, D. M. Tiede, Surface Restructuring of Nanoparticles: An Efficient Route for Ligand-Metal Oxide Crosstalk, *J. Phys. Chem. B.* 106 (2002) 10543–10552.

[16] N. M. Dimitrijević, Z. V. Šaponjić, B. M. Rabatic, O. G. Poluektov, T. Rajh, Effect of size and shape of nanocrystalline TiO_2 on photogenerated charges. An EPR Study, *J. Phys. Chem. C.* 111 (2007) 14597–14601.

[17] Z. V. Šaponjić, N. M. Dimitrijevic, D. M. Tiede, A. Goshe, X. Zuo, L. X. Chen, A. Barnard, P. Zapol, L. Curtiss, T. Rajh, Shaping nanometer-scale architecture through surface chemistry, *Adv. Mater.* 17 (2005) 965–971.

[18] C. Zhang, T. Uchikoshia, J. G. Li, T. Watanabe, T. Ishigaki, Photocatalytic activities of europium (III) and niobium (V) co-doped TiO_2 nanopowders synthesized in Ar/O_2 radio-frequency thermal plasmas, *J. Alloys. Comp.* 606 (2014) 37–43.

[19] W. Luo, R. Li, X. Chen, Host-Sensitized Luminescence of Nd^{3+} and Sm^{3+} Ions Incorporated in Anatase Titania Nanocrystals, *J. Phys. Chem. C.* 113 (2009) 8772–8777.

[20] M. Vranješ, J. Kuljanin-Jakovljević, S. P. Ahrenkiel, I. Zeković, M. Mitrić, Z. Šaponjić, J. M. Nedeljković, Sm^{3+} doped TiO_2 nanoparticles synthesized from nanotubular precursor luminescent and structural properties, *J. Lumin.* 143 (2013) 453–458.

[21] P. M. Kumar, S. Badrinarayanan, M. Sastry, Nano-crystalline TiO_2 Studied by Optical, FTIR and X-Ray Photoelectron Spectroscopy: Correlation to Presence of Surface States, *Thin Solid Films* 358 (2000) 122–130.

[22] K. L. Frindell, M. H. Bartl, M. R. Robinson, G. C. Bazan, A. Popitsch, G. D. Stucky, Visible and near-IR luminescence via energy transfer in rare earth doped mesoporous titania thin films with nanocrystalline walls, *Solid State Chem.* 172 (2003) 81–88.

[23] L. Hu, H. Song, G. Pan, B. Yan, R. Qin, Q. Dai, L. Fan, S. Li, X. Bai, Photoluminescence properties of samarium-doped TiO_2 semiconductor nanocrystalline powders, *J. Lumin*. 127 (2007) 371–376.

[24] V. Kiisk, I. Sildos, S. Lange, V. Reedo, T. Tätte, M. Kirm, J. Aarik, Photoluminescence characterization of pure and Sm^{3+}-doped thin metaloxide films, *App. Surf. Sci*. 247 (2005) 412–417.

[25] M. Kiisk, V. Savel, A. Reedo, Lukner, I. Sildos, Anatase-to-rutile phase transition of samarium-doped TiO_2 powder detected via the luminescence of Sm^{3+}, *Phys. Procedia.* 2 (2009) 527–538.

[26] N. Hong, W. Prellier, J. Sakai, A. Ruyter, Substrate effects on the room-temperature ferromagnetism in Co-doped TiO_2 thin films grown by pulsed laser deposition, *J. Appl. Phys*. 95 (2004) 7378–7380.

[27] J. Y. Kim, J. H. Park, B. G. Park, H. J. Noh, S. J. Oh, J. S. Yang, D. H. Kim, S. D. Bu, T. W. Noh, H. J. Lin, H. H. Hsieh, C. T. Chen, Ferromagnetism Induced by Clustered Co in Co-Doped Anatase TiO_2 Thin Films, *Phys. Rev. Lett.* 90 (2003) 017401.

[28] R. Kennedy, P. Stampe, E. Hu, P. Xion, S. von Molar, Y. Xin, Hopping transport in $TiO_{2:Co:}$ A signature of multiphase behavior, *Appl. Phys. Lett.* 84 (2004) 2832–2834.

[29] S. K. S. Patel, N. S. Gajbhiye, Room temperature magnetic properties of Cu-doped titanate, TiO_2(B) and anatase nanorods synthesized by hydrothermal method, *Mat. Chem. Phys.* 132 (2012) 175–179.

[30] N. H. Hong, J. Sakai, W. Prellier, Distribution of dopant in Fe:TiO_2 and Ni:TiO_2 thin films, *J. Magn. Magn. Mater.* 281 (2004) 347–352.

[31] M. Venkatesan, C. B. Fitzgerald, J. G. Lunney, J. M. D. Coey, Anisotropic Ferromagnetism in Substituted Zinc Oxide, *Phys. Rev. Lett.* 93 (2004) 177206.

[32] L. Yan, C. K. Ong, X. S. Rao, Magnetic order in Co-doped and (Mn, Co) codoped ZnO thin films by pulsed laser deposition, *J. Appl. Phys.* 96 (2004) 508–511.

[33] G. Dalpian, J. R. Chelikowsky, Self-Purification in Semiconductor Nanocrystals, *Phys. Rev. Lett*. 96 (2006) 226802.

[34] M. Vranješ, Z. Konstantinović, A. Pomar, J. Kuljanin Jakovljević, M. Stoiljković, J. M. Nedeljković, Z. Šaponjić, Room-temperature ferromagnetism in Ni^{2+} doped TiO_2 nanocrystals synthesized from nanotubular precursors, *J. Alloys Comp.* 589 (2014) 42–47.

[35] T. Ochiai, K. Masuko, S. Tago, R. Nakano, K. Nakata, M. Hara, Y. Nojima, T. Suzuki, M. Ikekita, Y. Morito, A. Fujishima, *Synergistic Water-Treatment Reactors Using a TiO_2-Modified Ti-Mesh Filter, Water.* 5 (2013) 1101–1115.

[36] M. V. Ganduglia-Pirovano, A. Hofmann, J. Sauer, Oxygen vacancies in transition metal and rare earth oxides: Current state of understanding and remaining challenges, *Surf. Sci. Rep.* 62 (2007) 219–270.

[37] M. You, T. G. Kim, Y. M. Sung, Growth of CdS Nanorod-Coated TiO_2 Nanowires on Conductive Glass for Photovoltaic Applications, *Cryst. Growth Des.* 9 (2009) 4519–4523.

[38] J. Wang, Q. W. Chen, C. Zeng, B. Y. Hou, Magnetic-Field-Induced Growth of Single-Crystalline Fe_3O_4 Nanowires, *Adv. Mater.* 16(2) (2004) 137–140.

[39] M. You, T. G. Kim, Y. M. Sung, Synthesis of Cu-Doped TiO_2 Nanorods with Various Aspect Ratios and Dopant Concentrations, *Cryst. Growth Des*. 10 (2010) 983–987.

[40] J. Kuljanin-Jakovljević, M. Radoičić, T. Radetić, Z. Konstantinović, Z. V. Šaponjić, J. Nedeljković, Presence of Room Temperature Ferromagnetism in Co^{2+} Doped TiO_2 Nanoparticles Synthesized through Shape Transformation, *J. Phys. Chem. C.* 113 (2009) 21029–21033.

[41] M. Vranješ, J. Kuljanin Jakovljević, Z. Konstantinović, A. Pomar, M. Stoiljković, M. Mitrić, T. Radetić, Z. Šaponjić, Shaped Co^{2+} doped TiO_2 nanocrystals synthesized from nanotubular precursor: Structure and ferromagnetic behavior, *J. Adv. Ceram.* 6 (2017) 220–229.

[42] M. Vranješ, J. Kuljanin-Jakovljević, Z. Konstantinović, A. Pomar, S. P Ahrenkiel, T. Radetić, M. Stoiljković, M. Mitrić, Z. Šaponjić, Room temperature ferromagnetism in Cu^{2+} doped TiO_2 nanocrystals: The impact of their size, shape and dopant concentration, *Mater. Res. Bull*. 76 (2016) 100–106.

[43] S. Turchi and D. F. Ollis, Photocatalytic degradation of organic water contaminants: Mechanisms involving hydroxyl radical attack, *J. Catal.* 122 (1990) 178–192.

[44] K. Konstantinou and T. A. Albanis, TiO_2-assisted photocatalytic degradation of azo dyes in aqueous solution: kinetic and mechanistic investigations: A review, *Appl. Catal. B: Environ.* 49 (2004) 1–14.

[45] M. Radoičić, Z. Šaponjić, I. A. Janković, G. Ćirić-Marjanović, S. P. Ahrenkiel, M. I. Čomor, Improvements to the photocatalytic efficiency of polyaniline modified TiO_2 nanoparticles, *Appl. Catal. B: Environ.* 136-137 (2013) 133–139.

[46] U. Riaz, S. M. Ashraf, J. Kashyap, Role of Conducting Polymers in Enhancing TiO_2-based Photocatalytic Dye Degradation: A Short Review, *Polym.-Plast. Technol.* 54 (2015) 1850–1870.

[47] U. Riaz, S. M. Ashraf, J. Kashyap, Enhancement of photocatalytic properties of transitional metal oxides using conducting polymers: A mini review, *Mater. Res. Bull.* 71 (2015) 75–90.

[48] K. R. Reddy, M. Hassan, V. G. Gomes, Hybrid nanostructures based on titanium dioxide for enhanced photocatalysis, *Appl. Catal. A: Gen.* 489 (2015) 1–16.

[49] G. Ćirić-Marjanović, I. Pašti, S. Mentus, One-dimensional nitrogen-containing carbon nanostructures, *Prog. Mater. Sci.* 69 (2015) 61–182.

[50] G. Ćirić-Marjanović, N. Pašti, A. Janošević, S. Mentus, Carbonised polyaniline and polypyrrole: towards advanced nitrogen-containing carbon materials, *Chem. Pap.* 67 (2013) 781–813.
[51] S. Mentus, G. Ćirić-Marjanović, M. Trchová, J. Stejskal, Conducting carbonized polyaniline nanotubes, *Nanotechnology.* 20(24) (2009) 245601.
[52] Y. Xu, Y. Mo, J. Tian, P. Wang, H. Yu, J. Yu, The synergistic effect of graphitic N and pyrrolic N for the enhanced photocatalytic performance of nitrogen-doped graphene/TiO_2 nanocomposite, *Appl. Catal. B: Environ.* 181 (2016) 810–817.
[53] G. Ćirić-Marjanović, M. Trchová, J. Stejskal, The chemical oxidative polymerization of aniline in water: Raman spectroscopy, *J. Raman Spec.* 39 (2008) 1375–1387.
[54] G. Ćirić-Marjanović, N. V. Blinova, M. Trchová, J. Stejskal, Evolution of Polyaniline Nanotubes: The Oxidation of Aniline in Water, *J. Phys. Chem. B* 110 (2006) 9461–9468.
[55] G. Ćirić-Marjanović, M. Trchová, E. N. Konyushenko, P. Holler, J. Stejskal, Chemical Oxidative Polymerization of Aminodiphenylamines, *J. Phys. Chem. B* 112(23) (2008) 6976–6987.
[56] M. B. Radoičić, M. Milošević, D. Miličević, E. Suljovrujić, G. Ćirić-Marjanović, M. Radetić, Z. Šaponjić, Influence of TiO2 nanoparticles on formation mechanism of PANI/TiO2 nanocomposite coating on PET fabric and its structural and electrical properties, *Surf. Coat. Technol.* 278 (2015) 38–47.
[57] M. Radoičić, Z. Šaponjić, J. Nedeljković, G. Ćirić-Marjanović, J. Stejskal, Self-assembled polyaniline nanotubes and nanoribbons/titanium dioxide nanocomposites, *Synth. Met.* 160 (2010) 1325–1334.
[58] J. Zhang, M. Li, Z. Feng, J. Chen, C. Li, UV Raman Spectroscopic Study on TiO_2. I. Phase Transformation at the Surface and in the Bulk, *J. Phys. Chem. B.* 110 (2006) 927–935.
[59] D. Regonini, A. Jaroenworaluck, R. Stevensa, C. R. Bowen, Effect of heat treatment on the properties and structure of TiO_2 nanotubes: phase composition and chemical composition, *Surf. Interface Anal.* 42 (2010) 139–144.
[60] M. Trchová, E. N. Konyushenko, J. Stejskal, J. Kovarova, G. Ćirić-Marjanović, The conversion of polyaniline nanotubes to nitrogen-containing carbon nanotubes and their comparison with multi-walled carbon nanotubes, *Polym. Degrad. Stab.* 94 (2009) 929–938.
[61] J. Robertson, Diamond-like amorphous carbon, *Mater. Sci. Eng. R.* 37 (2002) 129–281.
[62] T. Mazza, E. Barborini, P. Piseri, P. Milani, D. Cattaneo, A. Li Bassi, C.E. Bottani,C. Ducati, Raman spectroscopy characterization of TiO2 rutile nanocrystals, *Phys. Rev. B* 75 (2007) 045416.
[63] A. S. Attar, Z. Hassani, Fabrication and Growth Mechanism of Single-crystalline Rutile TiO_2 Nanowires by Liquid-phase Deposition Process in a Porous Alumina Template, *J. Mater. Sci. Technol.* 31 (2015) 828–833.
[64] D. Hurum, A. Agrios, K. Gray, T. Rajh, M. Thurnauer, Explaining the Enhanced Photocatalytic Activity of Degussa P25 Mixed-Phase TiO_2 Using EPR, *J. Phys. Chem. B.* 107 (2003) 4545–4549.
[65] M. Liu, L. Piao, L. Zhao, S. Ju, Z. Yan, T. He, C. Zhou, W. Wang, Anatase TiO_2 single crystals with exposed {001} and {110} facets: facile synthesis and enhanced photocatalysis, *Chem. Commun.* 46 (2010) 1664–1666.

[66] M. Radoičić, G. Ćirić-Marjanović, V. Spasojević, P. Ahrenkiel, M. Mitrić, T. Novaković, Z. Šaponjić, Superior photocatalytic properties of carbonized PANI/TiO_2 nanocomposites, *Appl. Catal. B: Environ.* 213 (2017) 155–166.
[67] R. Su, R. Bechstein, L. So, R. Vang, M. Sillassen, B. Esbjornsson, A. Palmqvist, F.Besenbacher, How the Anatase-to-Rutile Ratio Influences the Photoreactivity of TiO_2, *J. Phys. Chem. C.* 115 (2011) 24287–24292.
[68] Z. Xiong, H. Wu, L. Zhang, Y. Gu, X.S. Zhao, Synthesis of TiO_2 with controllable ratio of anatase to rutile, *J. Mater. Chem. A*. 2 (2014) 9291–9297.
[69] Z. Mou, Y. Wu, J. Sun, P. Yang, Y. Du, C. Lu, TiO_2 Nanoparticles-Functionalized N-Doped Graphene with Superior Interfacial Contact and Enhanced Charge Separation for Photocatalytic Hydrogen Generation, *ACS Appl. Mater. Interfaces.* 6 (2014) 13798–13806.
[70] P. Wang, Z. Wang, L. Jia, Z. Xiao, Origin of the catalytic activity of graphite nitride for the electrochemical reduction of oxygen: geometric factors *vs.* electronic factors, *Phys. Chem. Chem. Phys.* 11 (2009) 2730–2740.
[71] L. Yingliang, S. Wang, S. Xu, S. Cao, Evident improvement of nitrogen-doped graphene on visible light photocatalytic activity of N-TiO_2/N-graphene nanocomposites, *Mater. Res. Bull.* 65 (2015) 27–35.
[72] P. Wang, Y. Xia, P. Wu, X. Wang, H. Yu, J. Yu, Cu(II) as a General Cocatalyst for Improved Visible-Light Photocatalytic Performance of Photosensitive Ag-Based Compounds, *J. Phys. Chem. B.* 118 (2014) 8891–8898.

Марија Радоичић, Мила Врањеш, Јадранка Кузанин Јаковљевић, Гордана Ћирић Марјановић, Зоран Шапоњић

ИСПИТИВАЊЕ ОПТИЧКИХ, МАГНЕТНИХ И ФОТОКАТАЛИТИЧКИХ ОСОБИНА ДОПИРАНИХ TIO_2 НАНОКРИСТАЛА И НАНОКОМПОЗИТА НА БАЗИ ПОЛИМЕРА ЗА РАЗЛИЧИТЕ ПРИМЕНЕ

Р е з и м е

Испитиване су допиране и недопиране наночестице титан (IV) оксида (TiO_2), великог енергијског процепа, различитих облика (сферични, тубуларни, штапићасти (елипсоидни)), величина кристалних структура, као и хибридни материјали-нанокомпозити на бази проводног полимера (полианилин, ПАНИ) и наночестица TiO_2.

Испитивања утицаја величине, облика, структуре и нивоа допираности наночестица TiO_2 на њихове оптичке, магнетне и фотокаталитичке особине, као и разумевање интеракције наночестица и полимерне матрице (ПАНИ) у циљу креирања нанокомпозита одговарајућих фотокаталитичких својстава представљају главне правце овог истраживања.

Обзиром на структуру енергетског процепа наночестица TiO_2, допирање јонима ретких земаља отвара могућност за контролу њихових оптичких карактеристика. Нанокристали TiO_2 допирани јонима Sm^{3+} показују наранџасто-црвену емисију, која је последица *f-f* прелаза јона Sm^{3+} ($^4G_{5/2} \rightarrow {}^6H_J$ (J=5/2, 7/2 i 9/2)) и која потврђује постојање енергијског трансфера. Допирање наночестица TiO_2 јонима Ni^{2+} отвара могућност за синтезу транспарентних наноструктурних филмова који показују феромагнетно уређење на собној температури (H_C ~ 150-200 Oe) и сатурациону магнетизацију у опсегу 10^{-3}-$5x10^{-2}$ μ_B/Ni, у зависности од концентрације допанта.

Следећи циљ ових истраживања био је повећање фотокаталитичке ефикасности/активности наночестица TiO_2 површинском модификацијом проводним ПАНИ полимером у карбонизованој форми, уз дефинисање механизма процеса фотокаталитичке деградације модел молекула метиленско плавог (Methylene blue) и родамина Б (Rhodamine B). У поређењу са немодификованим наночестицама TiO_2, ПАНИ/TiO_2 нанокомпозити, ексцитовани белом светлошћу, показали су значајно већу фотокаталитичку ефикасност. Процес карбонизације полианилина у ПАНИ/TiO_2 нанокомпозитима је довео до даљег повећања њихове фотокаталитичке ефикасности. Фотокаталитичка активност нанокомпозита је условљена њиховом површинском структуром, високом мобилношћу носилаца наелектрисања и апсорпционим коефицијентом полианилина у видљивом делу спектра, као и молекулском структуром испитиваних боја.